

THESIS

CHEMICAL EQUILIBRIUM MODELING OF PHOSPHORUS REMOVAL AND
RECOVERY PROCESSES FOR ADVANCED WASTEWATER TREATMENT

Submitted by

Jinna Liu

Department of Civil and Environmental Engineering

In partial fulfillment of the requirements

For the Degree of Master of Science

Colorado State University

Fort Collins, Colorado

Spring 2018

Master's Committee:

Advisor: Kenneth Carlson

Sybil Sharvelle
Yaling Qian

Copyright by Jinna Liu 2018

All Rights Reserved

ABSTRACT

CHEMICAL EQUILIBRIUM MODELING OF PHOSPHORUS REMOVAL AND RECOVERY PROCESSES FOR ADVANCED WASTEWATER TREATMENT

Phosphorus (P) is a fundamental element to all life. However, unmanaged phosphorus can create negative effects in the environment. Wastewater is a significant source of phosphorus and every day, thousands of wastewater treatment and recovery facilities treat billions of gallons of nutrient rich wastewater. During the treatment process, a large amount of sludge is produced and needs to be treated and disposed. The main process for sludge treatment is anaerobic digestion after which the solids are dewatered. However, the dewatered sludge liquor or centrate contains very high levels of nutrients (nitrogen and phosphorus) that needs to be removed from this water stream before being returned to the secondary treatment process. This recycle stream adds additional nutrients to the plant which affects treatment efficiencies and increases operating costs. Additionally, when the phosphorus, magnesium and ammonia are released in the digester, they combine and can create struvite, a mineral that can cause significant damage to equipment, pumps and piping. In many cases, nutrient removal technologies are added in the sludge and centrate treatment process. This study used chemical equilibrium modeling to examine phosphorus removal and recovery in the centrate from dewatered anaerobic digestion sludge. The chemical equilibrium of two P recovery technologies (CNP's AirPrex P-recovery process, Ostara's Pearl® P-recovery process) and one P removal method (precipitation with ferric) are modeled using MINTEQ to understand how the overall water quality changes and how this could impact downstream processes. AirPrex and Pearl® produced struvite, which can be used as green fertilizer, have

several factors that influence the formation of product including pH, temperature and concentration of ions such as phosphorus, ammonia and magnesium.

One of the important differences between the AirPrex and Pearl® technologies is that AirPrex is installed between the anaerobic digestion and dewatering processes, while Pearl® is installed after dewatering. Through the model work, AirPrex could reach 98% P removal and 70% P recovery at the optimal situation from the digested sludge. Pearl® could reach 97% P removal and 96% P recovery at the optimal situation from centrate. The P removal method with ferric chloride could reach almost 100% phosphorus removal.

TABLE OF CONTENTS

ABSTRACT	ii
LIST OF TABLES	vi
LIST OF FIGURES	vii
CHAPTER 1. INTRODUCTION	1
1.1 Background.....	1
1.2 Problem statement	2
CHAPTER 2. BACKGROUND AND THEORY	5
2.1 Background of Phosphorus Treatment	5
2.2 Struvite.....	6
2.3 AirPrex and Pearl®	7
2.3.1 AirPrex	7
2.3.2 Pearl®.....	9
2.4 Chemistry of Precipitation.....	10
2.5 Activity correction.....	11
2.6 Possible Precipitate Solid	12
CHAPTER 3. METHODS/METHODOLOGY	15
3.1 Three Scenarios	15
3.1.1. Model I: P recovery method-AirPrex.....	15
3.1.2 Model II: P recovery method-Pearl®	16
3.1.3 Model III: P removal method with ferric chloride	17
3.2 Chemical Equilibrium Model	17
3.3 Calculation.....	21

3.3.1 Initial Data Calculation	21
3.3.2 Calculation for modeling.....	23
3.3.3 Calculation for results	24
CHAPTER 4. RESULTS DISCUSSION	26
4.1 AirPrex.....	26
4.2 Pearl® Process.....	34
4.2.1. Pearl® Process Model with pH=8.....	35
4.2.2. Pearl® Process Model with various pH	39
4.3 Ferric Chloride Addition	46
4.4 Comparison of Three P Recovery/Removal Methods.....	49
4.4.1 Amount of phosphorus recovery analysis	49
4.4.2 Additional chemical dose for three methods.....	51
CHAPTER 5. CONCLUSION.....	54
REFERENCES	56

LIST OF TABLES

Table 2.1: Possible precipitation solids and reactions	12
Table 3.1: Possible Solid and Solubility Product Constants.....	19
Table 3.2: Model Component and Related Species	24
Table 4.1: Constituent concentration in digested sludge	26
Table 4.2: AirPrex Parameter Sensitivity at Mg/P=0.8 for different temperatures.	31
Table 4.3: Water quality of centrate used in model	34
Table 4.4: Important information at Mg/P=1.0 with different temperature for Pearl® (pH=8)...	37
Table 4.5: Optimal P recovery information for three methods.....	50

LIST OF FIGURES

Figure 1.2: Ostara-Pearl ® Flow Scheme	3
Figure 2.1: AirPrex Reactor	8
Figure 2.2: Pearl® Reactor	9
Figure 3.1: Flow Scheme for model I	15
Figure 3.2: Flow scheme for model II	16
Figure 4.1: The ratio of equilibrium concentration in solution with initial concentration and precipitation (%) with various Mg:P ratios for significant ions in the AirPrex Process at 15°C .	28
Figure 4.2: Produced solid concentration in Airprex Process at 15°C	29
Figure 4.3: Signature Ion Concentration in Chemical Equilibrium for AirPrex.....	30
Figure 4.4: Carbonate losing in Airprex Process at 15°C.....	32
Figure 4.5: Alkalinity in 15°C 25°C and 35°C in Airprex Process	33
Figure 4.6: The ratio of equilibrium concentration in solution with initial concentration and precipitation (%) with various Mg and P ratios for significant ions in the Pearl® process at 15°C	35
Figure 4.7: Produced solid concentration in Pearl® Process at 15°C.....	36
Figure 4.8: Carbon Loss for Pearl® Process at pH=8 and 15°C	38
Figure 4.9: Alkalinity in 15°C 25°C and 35°C in Airprex Process	38
Figure 4.10: The ratio of equilibrium concentration in solution and initial concentration for Ca ²⁺ and PO ₄ ³⁻ with various Mg and P ratio under different pH in Pearl® Process	40
Figure 4.11: Four solid precipitation concentration with various Mg/P and different pH. (a) Calcite precipitated concentration. (b) Strengite precipitated concentration. (c) Struvite precipitated concentration. (d) Magnesite precipitated concentration.....	43

Figure 4.12: C loss with different pH values for the Pearl® process. 44

Figure 4.13: Alkalinity as CaCO₃ with different pH values for the Pearl® process 45

Figure 4.14: Calcium and phosphorus precipitation (%) in removal method with ferric chloride46

Figure 4.15: The amount of precipitated solid in removal method with ferric chloride..... 47

Figure 4.16: C loss for ferric chloride additional method..... 48

Figure 4.17: Alkalinity as CaCO₃ (mg/L) for ferric chloride additional method..... 48

Figure 4.18: Flow rates for AirPrex and Pearl® inflow (a) AirPrex (b)Pearl® 49

Figure 4.19: Additional chemical dose for three P removal methods..... 52

CHAPTER 1. INTRODUCTION

1.1 Background

Phosphorus plays an essential role to all life as it is present in key biomolecules such as deoxyribonucleic acid (DNA), ribonucleic acid (RNA), adenosine diphosphate (ADP), adenosine triphosphate (ATP) and phospholipids. It can be said that without it, no life as we know it would exist. In nature, phosphorus is present as orthophosphate (OP) normally and most phosphates originate in ocean sediments or in rocks. In the phosphorus cycle, the phosphate in ocean sediments transfers to the soil or rock on the land through geologic processes and plants absorb phosphates from soil and plants are eaten by herbivores that proceed up the food chain. After animal and plant death, their body decays and returns phosphate back to the soil (The Environmental Literacy Council, 2015). Runoff or weathering may carry them back to the ocean or be incorporated into rock. The phosphorus cycle is one of the slowest material cycles in nature and unmanaged phosphorus can create serious consequences for the environment. The use of commercially available synthetic fertilizer can impact the phosphate cycle because plants may not utilize all of the phosphate from fertilizer and the excess can be transported to lakes with water run-off. Therefore, urban runoff and non-agricultural rural run-off can be large nonpoint phosphorus sources, and municipal and industrial wastewater treatment facilities are important point sources of phosphorus. Therefore, under human influence, much of the phosphate that accumulates in water is through point and non-point sources and the level can exceed natural phosphorus self-recovery ability and cause several problems to water quality and the environment. Phosphorus accumulation causes eutrophication and can disrupt the aqueous ecological balance. Excessive algal and bacterial growth in lakes and reservoirs leads to over-consumption of oxygen in water

leading to fish and other aquatic life death. Eutrophication or excessive productivity in the water column can lead to taste and odor issues and increases the cost and difficulty for water purification.

Every day, thousands of wastewater treatment and recovery facilities treat billions of gallons of wastewater which contain high nutrient levels. One method for removing phosphorus uses ferric salts (e.g. FeCl_3) to precipitate ferric phosphate followed by solid liquid separation in a settling and/or filtration process. A downside of ferric precipitation is operating and capital costs that include managing the solids that result from the process and the recurring chemical expenses. The main process used to stabilize and reduce the volume of wasted activated sludge is anaerobic digestion usually followed by a dewatering process. Anaerobic digestion transforms organic matter into biogas destroying most of the pathogens in sludge. Besides reducing sludge volume, this process also limits odor problems but also contains a high amount of inorganic phosphorus and magnesium. In the subsequent dewatering process, centrifugation can be used to produce solid cake and with a by-product liquid centrate stream. The centrate stream will be recycled back to the secondary treatment influent stream adding additional nutrient loading to the plant and potentially affecting the treatment efficiency and increasing operating costs. In addition, with high concentrations of magnesium, ammonium and phosphorus ions, struvite (MgNH_4PO_4) scale deposit can cause problems for operation.

1.2 Problem statement

Uncontrolled struvite formation inside wastewater treatment plant infrastructure can affect the efficiency of treatment and increase the cost for maintenance. Managed struvite formation can reduce maintenance cost and produce fertilizer quality products. Today, struvite crystallization is a technology used for phosphorus recovery which forms struvite under a controlled environment. In this study, there are two P recovery technologies that were evaluated, Airprex from CNP

Technology Water and Biosolid Corporation and the Pearl® process from Ostara Nutrient Recovery Technology Inc. Those two technologies both work for waste activated sludge treatment. AirPrex is installed between the anaerobic digester and the dewatering equipment in a sludge liquid treatment process and Pearl® is installed after the anaerobic digester and dewatering equipment. Increasingly, deammonification processes using Anammox bacteria are being deployed downstream of P-recovery process and are sensitive to the inorganic water quality, particularly the concentration of inorganic carbon and therefore upstream processes may have a significant influence.

Figures 1.1 and 1.2 show simple flow schematics of the AirPrex and Pearl® processes.

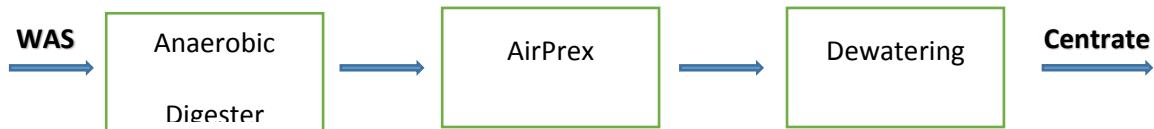


Figure 1.1: CNP-AirPrex Flow Scheme

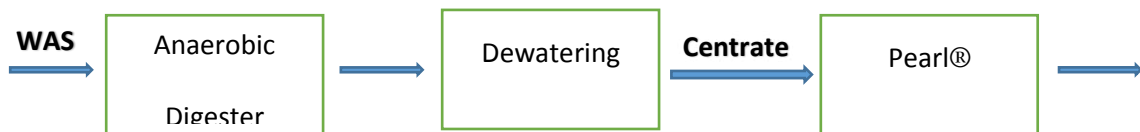


Figure 1.2: Ostara-Pearl® Flow Scheme

During anaerobic digestion, organic phosphorus (P in organic molecules) is mineralized and converted to inorganic phosphorus (e.g. ortho-phosphate) which is then available for assimilation by aquatic organisms. High concentrations of orthophosphate, magnesium and ammonia in the aqueous phase can provide the necessary condition for struvite precipitation. This study compared and evaluated two pre-dewatering and one post-dewatering technologies with chemical equilibrium models. Two of technologies (AirPrex and Pearl) are relatively new processes that are

designed to recover P in the form of struvite. These processes were compared to a more traditional method for P removal, the addition of ferric chloride to precipitate ferric phosphate, to assess the potential impact on downstream processes such as *Anammox* deammonification.

The objectives of this study are:

1. Model and simulate chemical equilibrium for P recovery process.
2. Compare P recovery for pre-dewatering technology, post-dewatering technology and P recovery with ferric chloride.
3. Understand inorganic carbon fate through the P recovery and removal processes.

CHAPTER 2. BACKGROUND AND THEORY

This chapter first provides the background of phosphorus treatment and a general introduction to phosphorus recovery and removal methods. Then, the chapter gives the information about struvite which is main product of the phosphorus recovery methods, AirPrex and Pearl®, which are modeled in the study. Next, the general chemical reactions and equations about precipitation are given and methods for activity correction are introduced. The possible precipitate solids are discussed in the last section of this chapter.

2.1 Background of Phosphorus Treatment

Phosphorus is essential to life but unmanaged it can negatively affect water quality and the environment. Sometimes, uncontrolled phosphorus could cause destructive consequences to an aquatic system as P compounds in a lake may be chemically or enzymatically hydrolyzed to orthophosphate which could be assimilated by bacteria, algae and plants. In the bottom of a lake, many microbial communities use many of the organic constituents of sediment and release P contents back to water as orthophosphate. If there is excess phosphorus in the water, algae, bacteria and plants at the water surface grow rapidly with the bottom layer of water (hypolimnion) often becoming anoxic and much of P in sediments is released and diffuses back into water (Correl, 1998). As more phosphorus accumulates in the water, the anoxic conditions impact fish and other aquatic life populations and can even result in conditions that reduce sulfate (SO_4^{-2}) to sulfide (HS^-) a very undesirable form of sulfur.

Since the 1950s, phosphorus removal technologies have been developed to address the issue of rampant eutrophication (Morse, 1998). Initially, chemical precipitation methods were used to remove phosphorus using a physico-chemical process (precipitation followed by solid separation).

This process needs the addition of a metal salt, usually either iron or aluminum which are added as chlorides or sulfate and produce phosphorus as metal salt in waste sludge (Morse, 1998). Chemical precipitation has some problems including chemicals are expensive excessive chemical sludge production also adds to costs. Also, phosphate form a metal phosphate with an adhered water fraction, so the precipitant is less dewaterable. With the associated water, the amount of sludge that needs to be managed sludge is large and costly to dispose of. Recently, more and more treatment plants are choosing to use biological removal methods developed in the late 1950s (Janssen, 2002. Morse, 1998). Biological removal uses bacteria known as phosphorus accumulating organisms or PAOs. PAOs remove phosphate by accumulating it in cells as polyphosphate and release it in digester of waste activated sludge treatment process.

2.2 Struvite

In 1939, treatment plant personnel found crystalline material in pipes that was identified as struvite with a purity of 96% (Jame,2002). He pointed out that CO₂ evolution through pipe fitting increases the pH which enhanced the struvite deposition. In 1963, operators at Hyperion treatment plant in Los Angeles found that struvite deposits on the underside of digestion screens leading to diluting the digested sludge stream to prevent the problem (Jame,2002). In 1972, Borgerding confirmed struvite as a source of scale deposits in the wastewater treatment plants. This scale problem was solved by an acidic treatment firstly, but it reappeared a few years later and blocked the pipes in the same plant (Le Corre, 2009). These events led to an increased interest in the occurrence of struvite.

Struvite, chemical name magnesium ammonium phosphate hexahydrate, is a white crystal that has an orthorhombic structure with regular PO₄³⁻ octahedral, distorted Mg(H₂O)₆²⁺ octahedral, and NH₄ groups all held by hydrogen bonding (Le Corre, 2009). The molecular weight is 245 g*mol⁻¹

¹. Struvite has low solubility in water (0.018 g*100 ml⁻¹ at 25°C), however, in acids, struvite has a higher solubility, 0.033 g*100 ml⁻¹ in 0.001 eq/L HCl at 25°C and 0.178 g*100 ml⁻¹ in 0.01 eq/L HCl at 25°C (Le Corre, 2009).

Struvite consists of magnesium, ammonium and phosphorus. Struvite precipitates following the general equation with n=0, 1 or 2 (Le Corre, 2009).



This is a simplified equation of the chemistry related to struvite precipitation. Like all crystallization processes, struvite precipitation can be divided into two stages: nucleation and growth (Jame, 2002). During nucleation, crystal embryos are formed with constituent ions combining. Then, crystal growth continues until reaching equilibrium. In equilibrium, struvite crystallization is in balance with dissolution of the crystals. So, in the system where continuously replenished with struvite constituents, crystal growth may continue indefinitely (Jame,2002).

There is a combination of factors related to struvite precipitation which include the crystal state of initial compounds, liquid-solid equilibrium thermodynamics, solid and liquid phase matter transfer, reaction kinetics, and physico-chemical parameters such as pH, supersaturation ratio, mixing energy, temperature and presence of foreign ions (Le Corre, 2009).

2.3 AirPrex and Pearl®

2.3.1 AirPrex

The AirPrex process was developed to prevent unwanted struvite after digestion in WWTP which is directly after the digester in the sludge phase of WWTPs with enhanced biological phosphorus removal (EBPR) and prior to sludge dewatering. The reactor of AirPrex is an airlift reaction where air is pressed in through the bottom and released through top. With CO₂ stripping,

pH is increased which reduces the additional chemicals for adjusting pH. The figure 2.1 below shows the reactor of AirPrex which from Gerhard Forstner presentation.

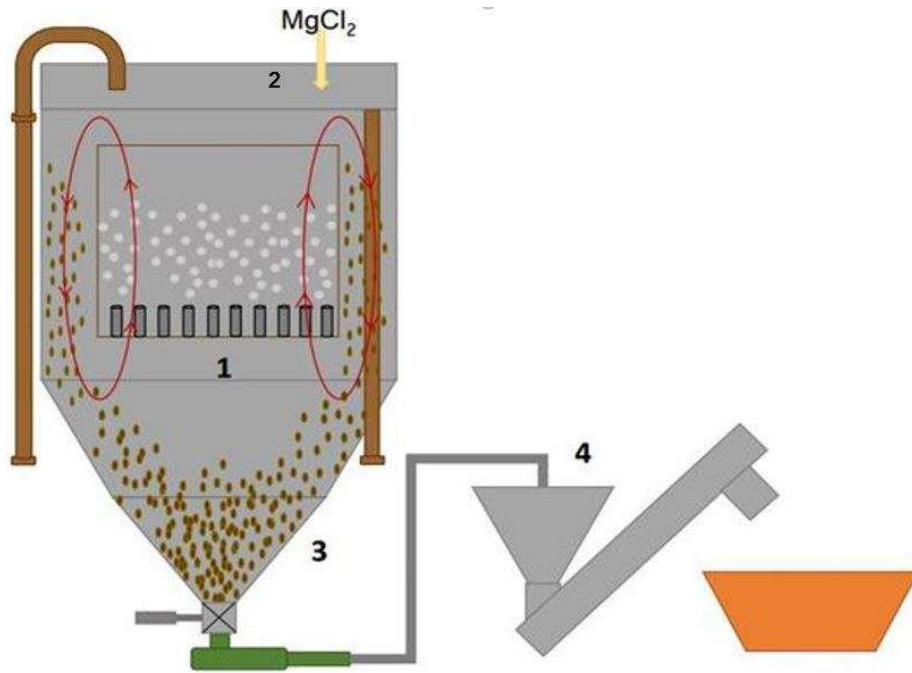


Figure 2.1: AirPrex Reactor

In the reactor, there is a cylindrical wall which dividing the reactor into two parts, central part and outer part. Sludge is moving upward in the central part and flowing down in the outer ring. Phosphorus and ammonia in sludge contact with magnesium which is added in the process. In the streaming loop, chemical reactants have a good contact and struvite formation and crystals growth in the looping. When the crystal grows to a sufficient size, MAP will accumulate as sediment in the bottom of the reactor where struvite can be extracted. At the same time, the sludge leaves the system through the top of reactor's outer part and goes to dewatering step.

Because AirPrex is installed immediately after the digester, it reduces the problem of pipe blocking. From the website of CNP, AirPrex can reduce up to 90% of the phosphate recycle load,

reduce maintenance costs by up to 50%, reduce up to 30% polymer consumption, reduce up to 20% disposal costs and produce significant fertilizer revenue.

2.3.2 Pearl®

The Ostara Pearl® reactor is a fluidized bed which is an up-flow reactor with several level diameters. Pearl® is installed after the dewatering process. From the Ostara website, up to 50% total influent phosphorus could be removed which reduces the struvite accumulation in pipes and other infrastructure. A schematic of the Pearl® reactor is shown below.

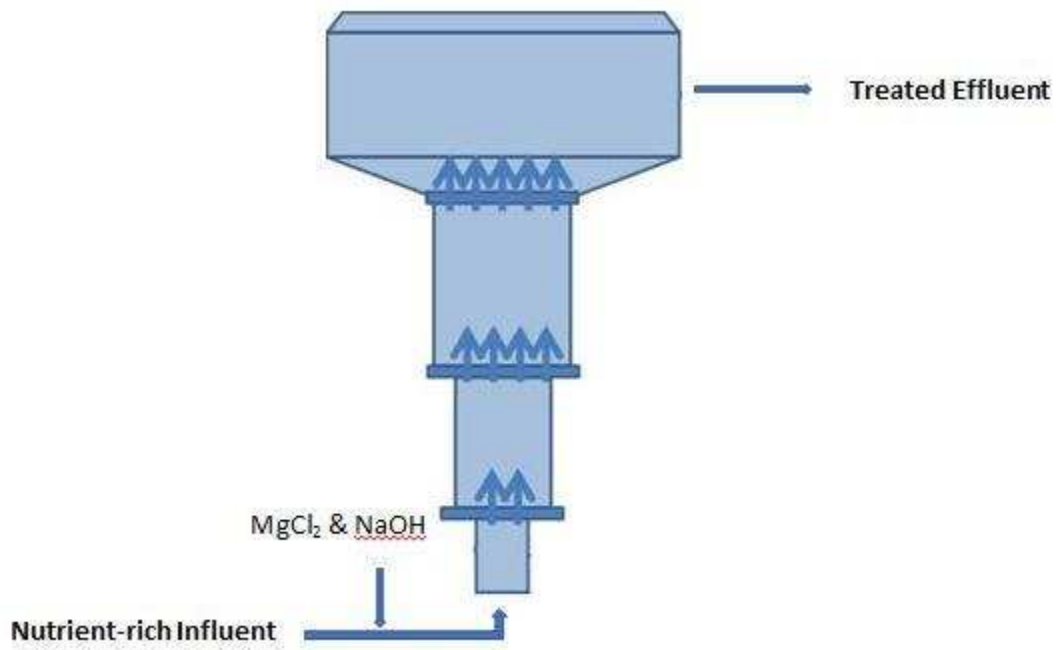


Figure 2.2: Pearl® Reactor

In the reactor, the digester supernatant flows upwards as growing struvite crystals fill in the reactor. The chemicals such as MgCl₂ and caustic soda (NaOH) are added from the bottom of the reactor. In the lowest cylindrical part, the digester supernatant is separated from sludge with centrifugation and dosed into the dosing zone of the Pearl® reactor. Then struvite crystals will grow and precipitate in the reactor and be collected in the bottom. The upper part of reactor is

designed as a clarifier with a weir overflow. Solid-free liquid is separated and recycled from the top.

2.4 Chemistry of Precipitation

The general equation of dissolution in water is:



The solubility product constant K_{sp} is:

$$K_{sp} = [A^{n+}]_{eq}^a * [B^{n-}]_{eq}^b \quad (2.3)$$

Where $[A^{n+}]_{eq}$ and $[B^{n-}]_{eq}$ are the concentration of ions in equilibrium, and a and b are the valences of the ions.

The ion activity product (IAP) is:

$$IAP = [A^{n+}]_{actual}^a * [B^{n-}]_{actual}^b \quad (2.4)$$

Compared with K_{sp} , IAP uses real ion concentrations in water which describes the non-equilibrium state.

The saturation index(SI) is used to determine whether the water is saturated, undersaturated or supersaturated.

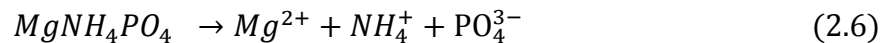
$$SI = \log_{10} \left(\frac{IAP}{K_{sp}} \right) \quad (2.5)$$

When $SI=0$, which means $IAP = K_{sp}$. The mineral is saturated.

When $SI<0$, which means $IAP < K_{sp}$. The mineral is undersaturated.

When $SI>0$, which means $IAP > K_{sp}$. The mineral is supersaturated.

For struvite, applying equation (2.3) to struvite dissolution (2.6):



$$K_{sp} = \{Mg^{2+}\} * \{PO_4^{3-}\} * \{NH_4^+\} \quad (2.7)$$

At 25 Celsius, from the database of Visual MINTEQ, struvite solubility product value (K_{sp}) is $5.5e-14$.

2.5 Activity correction

In high concentration(C_i) solutions, the activity of ions, or the effective concentrations, is less than the actual concentration due to charge-charge interactions. Equilibrium constants calculated are expressed in terms of ion effective concentration which is the activity. In the other words, activity is the ion concentration available for reaction. Activity is defined as:

$$Activity(a_i) = Effective\ concentration \quad (2.8)$$

Ideal Solution: $a_i = C_i$

Non-ideal solution: $a_i < C_i$

The expression for activity is:

$$a_i = \gamma_i \times m_i \quad (2.9)$$

Where γ_i is free ion activity coefficient and m_i is molar concentration of the free ion.

γ_i (free ion activity coefficient) describes the relation between the activity and concentration of free ion species. γ_i can obtain from Davies, Debye-Huckel equations and SIT method depending on ionic strength(I)

Ionic strength is a measure of the total ion concentration in solution as defined in Eq 10.

$$I = \frac{1}{2 \sum m_i \times Z_i^2} \quad (2.10)$$

Where m_i is concentration of ith ion and Z_i is charge of ith ion.

For free ion activity coefficients.

1. Debye-Huckel equation:

$$\log \gamma_i = -AZ_i^2 I^{\frac{1}{2}} \quad (2.11)$$

Where A is constant which is value of 0.51 at 25°C.

The range of this equation is limited to $I < 0.01$.

2. Extended Debye-Huckel equation:

$$\log \gamma_i = - \frac{AZ_i^2 I^{1/2}}{1 + a_i \times B \times I^{1/2}} \quad (2.12)$$

Where A and B are constants. $A=0.51$ and $B=0.33e8$ for 25°C water.

The range of this equation application is $I < 0.1$.

3. Davies

$$\log \gamma_i = -AZ_i^2 \left\{ \frac{I^{1/2}}{1 + I^{1/2}} - 0.2I \right\} \quad (2.13)$$

This equation is applicable when $I < 0.5$.

4. SIT(specific interaction theory) is applicable when $0.5 < I < 3$.

2.6 Possible Precipitate Solid

The aqueous digester centrate solution contains magnesium, calcium, ammonia, phosphate and inorganic carbon which are likely to precipitate. Table 2.1 shows the possible species and their reactions from literature.

Table 2.1: Possible precipitation solids and reactions

Minerals	Reaction
Struvite	$MgNH_4PO_4 \cdot 6H_2O \leftrightarrow Mg^{2+} + NH_4^+ + PO_4^{3-} + 6H_2O$
Newberyite	$MgHPO_4 \cdot 3H_2O \leftrightarrow Mg^{2+} + HPO_4^{2-} + 3H_2O$
Bobierite	$Mg_3(PO_4)_2 \cdot 8H_2O \leftrightarrow 3Mg^{2+} + 2PO_4^{3-} + 8H_2O$
Brushite	$CaHPO_4 \cdot 2H_2O \leftrightarrow Ca^{2+} + HPO_4^{2-} + 2H_2O$
Monenite	$CaHPO_4 \leftrightarrow Ca^{2+} + HPO_4^{2-}$

Hydroxyapatite	$Ca_{10}(PO_4)_6(OH)_2 \leftrightarrow 10Ca^{2+} + 6PO_4^{3-} + 2OH^-$
Tricalcium Phosphate	$Ca_3(PO_4)_2 \leftrightarrow 3Ca^{2+} + 2PO_4^{3-}$
Nesquehonite	$MgCO_3 \cdot 3H_2O \leftrightarrow Mg^{2+} + CO_3^{2-} + 3H_2O$
Magnesite	$MgCO_3 \leftrightarrow Mg^{2+} + CO_3^{2-}$
Calcite	$CaCO_3 \leftrightarrow Ca^{2+} + CO_3^{2-}$
Dolomite	$CaMg(CO_3)_2 \leftrightarrow Ca^{2+} + Mg^{2+} + 2CO_3^{2-}$
Huntite	$CaMg_3(CO_3)_4 \leftrightarrow Ca^{2+} + 3Mg^{2+} + 4CO_3^{2-}$
Calcium hydroxide	$Ca(OH)_2 \leftrightarrow Ca^{2+} + 2OH^-$
Magnesium hydroxide	$Mg(OH)_2 \leftrightarrow Mg^{2+} + 2OH^-$
Ferric phosphate	$FePO_4 \leftrightarrow Fe^{3+} + PO_4$
Vivianite	$Fe_3(PO_4)_2 \cdot 8H_2O \leftrightarrow 3Fe^{2+} + 2PO_4^{3-} + 8H_2O$

From Table 2.1 there are three possible magnesium phosphate species; struvite, newberyite and bobierite. Struvite precipitates at pH 7-11 (Corre,2009), Newberyite precipitation occurs at a lower pH (<6) and at high Mg and P concentrations (Turker,2010). Bobierite has a very low precipitation rate which was considered insignificant for the modeling exercise.

For calcium phosphate species, four crystalline species can precipitate; brushite, hydroxyapatite, tricalcium phosphate and octacalcium phosphate. Brushite precipitates at pH<7 whereas Octacalcium phosphate is formed by hydrolysis of brushite at pH 5~6 (Celen, 2007). Celen (2007) also reported the kinetics of tricalcium phosphate and hydroxyapatite precipitation process are extremely slow and likely occur mainly in geologic systems. Also, the magnesium ion hinders hydroxyapatite and octacalcium phosphate nucleation and growth. So, hydroxyapatite, tricalcium phosphate and octacalcium phosphate were not considered as potential solids for the modeling exercise.

For carbonate species, with calcium and magnesium, the possible precipitation solids are magnesite, calcite, nesquehonite, dolomite and huntite. There are some other salts possible precipitation which include magnesium hydroxide and calcium hydroxide and salts related to iron such as ferric phosphate and vivianite (Mamais, 1994 & Musvoto, 2000). Calcium hydroxide and magnesium hydroxide precipitation were not considered because they only occur at high pH values.

CHAPTER 3. METHODS/METHODOLOGY

This chapter introduces three phosphorus recovery or removal scenarios which form the three separate parts of the modeling work. The difference of these three scenarios is described and the flow schemes presented and discussed in this chapter. Also, the chemical equilibrium model, Visual MINTEQ is introduced and information is provided about the set-up and execution of the model. The parameters and constants used in the model are also discussed.

3.1 Three Scenarios

Three P recovery or removal methods were studied and modeled.

3.1.1. Model I: P recovery method-AirPrex

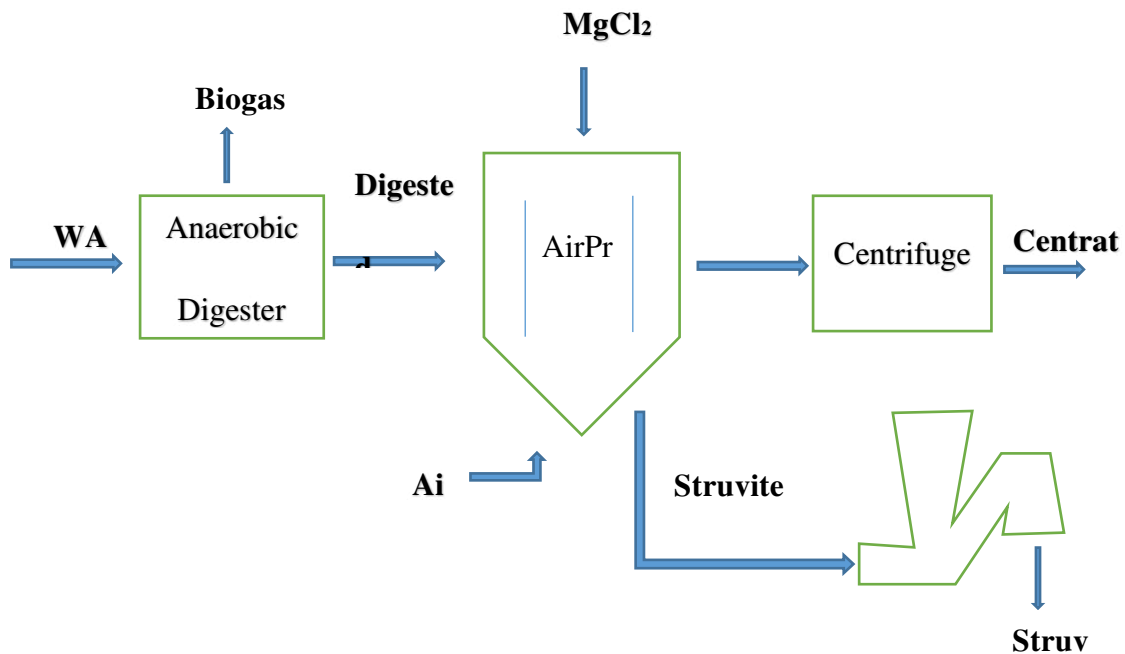


Figure 3.1: Flow Scheme for model I

AirPrex is installed between anaerobic digestion and the sludge dewatering process. The wasted activated sludge releases high concentrations of phosphorus and magnesium in the

anaerobic digester. The digested sludge flows into the Airprex reactor where it is exposed to an aeration process. Air is pumped in from the bottom of reactor and CO₂ is stripped out, increasing the pH. Since magnesium is the limiting reactant for the precipitation of struvite, the Aiprex process includes the addition of magnesium chloride into the reactor. The modeling exercise investigated the optimal P recovery versus MgCl₂ concentration for digested sludge.

3.1.2 Model II: P recovery method-Pearl®

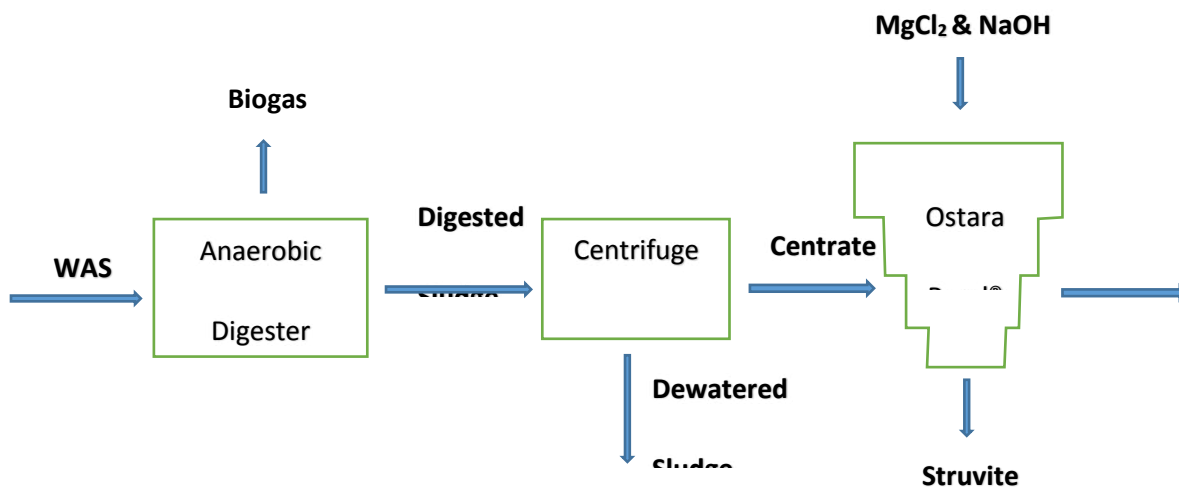


Figure 3.2: Flow scheme for model II

Pearl® is installed after dewatering process to treat the liquid phase or centrate from a centrifuge in this study. WAS through anaerobic digestion produces sludge with high concentrations of phosphorus and magnesium and after the digester, the effluent flows to the centrifuge for dewatering which continues flow into the Ostara Pearl® reactor. Besides magnesium chloride, caustic soda is added to adjust pH in the process. There are three steps for setting up Model II (Pearl).

Step I: investigate optimal P recovery with MgCl₂ concentration for centrate under assuming an initial pH=8.

Step II: adjust pH using caustic soda to 9, 10, and 11, and calculate the concentration of NaOH added for each pH.

Step III: investigate optimal P recovery with $MgCl_2$ concentration for centrate assuming pH=9, 10 and 11.

3.1.3 Model III: P removal method with ferric chloride

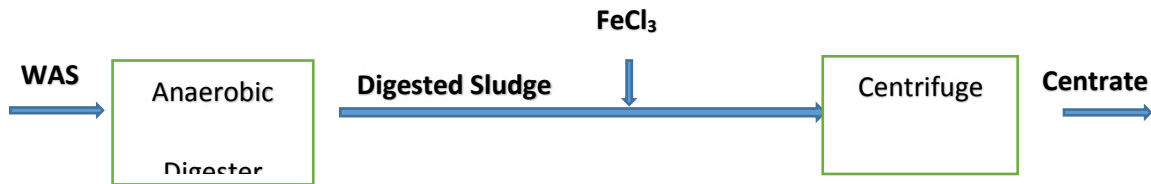


Figure 3.3: Flow scheme for model III

P removal using ferric chloride does not produce struvite but precipitates ferric phosphate ($FePO_4$). This method is used to compare the phosphorus removal efficiency with the two phosphorus recovery technologies described previously. This process is after anaerobic digestion process and the only chemical added ferric chloride ($FeCl_3$). Model III investigated the optimal P recovery with $FeCl_3$ for the digested sludge.

3.2 Chemical Equilibrium Model

This research used the chemical equilibrium model, Visual MINTEQ 3.1 which can be used to compute the composition of aqueous solutions in the laboratory or in natural water by calculating the solid phase, gas phase, adsorption and redox equilibria. The code of Visual MINTEQ is based on MINTEQA2 software developed by the U.S. Environmental Protection Agency.

The Visual MINTEQ protocol involves the following elements.

1. Determine default settings.

There are three methods for activity correction to select from.

- a. Davies
- b. Debye-Huckel
- c. SIT(Specific Ion Interaction)

From the literature review, Debye-Huckel is applicable for $I < 10^{-2}$. Davies is applicable for $I < 0.5$. SIT method is fit on $0.5 < I < 3$. Through calculation, the ionic strength of digested sludge is 0.25 and the ion strength of centrate is 0.09 and therefore the Davies method was chosen.

There are three choices for treating precipitation reactions.

- a. Oversaturated solids are not allowed to precipitate.
- b. Oversaturated solids are allowed to precipitate, but only after the final answer is reached.
- c. Oversaturated solids are allowed to precipitate each time a mineral precipitates or dissolves.

There is some mineral species in the Visual MINTEQ database that need long precipitation periods on the order of months or years. Since precipitation of these minerals will not occur in the reactor times discussed in this study, the possible solids were limited based on literature derived information. In this case, the oversaturated solids are not allowed to precipitate.

2. Set pH and ionic strength

There are two choices about pH and ionic strength which are fixed and not fixed. For this study, pH and ionic strength are not fixed and were calculated from mass and charge balances.

3. Enter temperature.

Three different temperatures were modeled: 15°C, 25°C and 35°C.

4. Input the system components and their concentrations.

Much of the data for water and solids quality came from experimental values collected from the Denver Metropolitan Wastewater Reclamation District (MWRD). MWRD conducted pilot testing of Ostara's Pearl® Phosphorus Recovery Process AirPrex technology at the Robert W. Hite Treatment Facility (RWHTF) in 2015 and the AirPrex technology was pilot tested in 2016. Those values depend on the initial data of digested sludge and centrate and the amount of additional chemicals added.

5. Edit the possible solid phase.

If in the default settings, check that oversaturated solids are not allowed to precipitate. The possible solid was edited based on equilibrium constants. Table 3.1 shows the possible solid in the model and their Ksp values.

Table 3.1: Possible Solid and Solubility Product Constants

<i>Possible Solid</i>	<i>Formula</i>	<i>Log (Ksp)</i>
-----------------------	----------------	------------------

<i>Brushite</i>	$\text{CaHPO}_4 \cdot 2\text{H}_2\text{O}$	-6.6
<i>Calcite</i>	CaCO_3	-8.48
<i>Huntite</i>	$\text{CaMg}_3(\text{CO}_3)_4$	-29.97
<i>Magnesite</i>	MgCO_3	-7.46
<i>Nesquehonite</i>	$\text{MgCO}_3 \cdot 3\text{H}_2\text{O}$	-24.22

<i>Newberyite</i>	$\text{MgHPO}_4 \cdot 3\text{H}_2\text{O}$	-18.18
<i>Siderite</i>	FeCO_3	-10.7
<i>Strengite</i>	$\text{FePO}_4 \cdot 2\text{H}_2\text{O}$	-26.4
<i>Struvite</i>	$\text{MgNH}_4\text{PO}_4 \cdot 6\text{H}_2\text{O}$	-13.26
<i>Vivianite</i>	$\text{Fe}_3(\text{PO}_4)_2 \cdot 8\text{H}_2\text{O}$	-37.76

6. Specify the gases

For the system studied, there are two dissolved gases in water that need to be accounted for, ammonia (NH_3) and carbon dioxide (CO_2). Ammonia has a high solubility in the water when it is the acid form (NH_4^+), so most of the ammonia produced will stay in water if the pH is less than the $\text{NH}_4^+ \rightleftharpoons \text{NH}_3$ pK_a value of 9.3. For carbon dioxide, the partial pressure needed to be input to the model. Because the phosphorus recovery is an aeration process, the partial pressure of CO_2 can be assumed to be that of the atmosphere. In the atmosphere, the partial pressure of carbon dioxide is 0.038% (400 ppm) and the log partial pressure as value $\log(0.038\%) = -3.42$.

7. Run the model

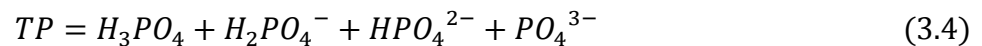
It is a loop process. Visual MINTEQ run out the results with input components concentration. So, component concentrations need to keep adjusting depending on the amount of additional chemicals and multiple model runs are accomplished across a range of the input parameters including temperature and pH.

3.3 Calculation

3.3.1 Initial Data Calculation

Raw data was collected from pilot testing at the Colorado State University Environmental Engineering labs including concentrations of the following parameters: calcium, iron, magnesium, potassium, sodium, ammonia and phosphorus, total alkalinity, pH and temperature. For digested sludge, MWRD collected data each seven days from Jun.15 – Aug.3 in 2016. The average values of the data (n=8) are used for analysis. For raw data of centrate, MWRD provided the table of four month average data for most of ion concentrations and CSU lab collected eighteen data from Apr.5 – Jul.16 in 2016. The four month average data is mainly used in analysis with CSU lab data as supplementary data. The aqueous concentrations of carbonate, bicarbonate, phosphate, hydrogen phosphate and chloride were determined using the following protocol.

Step1. Calculated PO_4^{3-} , HPO_4^{2-} and $H_2PO_4^-$ with known pH and total phosphorus concentration using the Solver Tool in Excel and the following equations:



Because the concentration of H_3PO_4 is too low in neutral and alkaline environment, it will be neglect in calculation. In excel file, enter the concentration of PO_4^{3-} and $H_2PO_4^-$ as the function of HPO_4^{2-} and the total phosphorus as the function of PO_4^{3-} , HPO_4^{2-} and $H_2PO_4^-$.

$$[PO_4^{3-}] = \frac{[HPO_4^{2-}] \times k_{a3}}{[H^+]} \quad (3.5)$$

$$[H_2PO_4^-] = \frac{[HPO_4^{2-}] \times [H^+]}{k_{a2}} \quad (3.6)$$

$$TP = [H_2PO_4^-] + [HPO_4^{2-}] + [PO_4^{3-}] \quad (3.7)$$

Total phosphorus is known from the collected raw data. Set total phosphorus as objective to raw value and the concentration of hydrogen phosphate as changing value. Using Solver Tool in Excel, the concentration of $H_2PO_4^-$, HPO_4^{2-} and PO_4^{3-} are calculated.

Step 2. Calculate H_2CO_3 , HCO_3^- and CO_3^{2-} with known pH, alkalinity and calculated phosphate, hydrogen phosphate and dihydrogen phosphate concentration using Solver Tool in Excel and the equations:



$$\text{Alk} \left(\frac{\text{eq}}{\text{L}} \right) = [HCO_3^-] + 2 [CO_3^{2-}] + [HPO_4^{2-}] + 2 \times [PO_4^{3-}] + [OH^-] \quad (3.10)$$

In excel file, enter the concentration of CO_3^{2-} and H_2CO_3 as the function of HCO_3^- and alkalinity as the function of HCO_3^- , CO_3^{2-} , PO_4^{3-} , HPO_4^{2-} and OH^- .

$$[CO_3^{2-}] = \frac{[HCO_3^-] \times k_{a2}}{[H^+]} \quad (3.11)$$

$$[H_2CO_3] = \frac{[HCO_3^-] \times [H^+]}{k_{a1}} \quad (3.12)$$

$$\text{Alk} \left(\frac{\text{eq}}{\text{L}} \right) = [HCO_3^-] + 2 [CO_3^{2-}] + [HPO_4^{2-}] + 2 \times [PO_4^{3-}] + [OH^-] \quad (3.13)$$

Alkalinity is known from raw data and concentration of phosphate, hydrogen phosphate and dihydrogen phosphate are calculated in Step 1. Set alkalinity as objective to raw value and the concentration of bicarbonate as changing value. Using Solver Tool in Excel, the concentration of CO_3^{2-} , HCO_3^- and H_2CO_3 are calculated.

Step 3. Calculated Cl^- with a charge balance equation with all known ion concentrations.

$$\begin{aligned}
& [NH_4^+] + 2 * [Ca^{2+}] + 3 * [Fe^{3+}] + [K^+] + 2 * [Mg^{2+}] + [Na^+] + [H^+] \\
& = [HCO_3^-] + 2 * [CO_3^{2-}] + [H_2PO_4^-] + 2 * [HPO_4^{2-}] + 3 * [PO_4^{3-}] + [Cl^-] \\
& + 2 * [SO_4^{2-}] \quad (3.14)
\end{aligned}$$

3.3.2 Calculation for modeling

Visual MINTEQ could compute the composition of the aqueous solution in the lab or in natural water. But it need to add components at the first steps. The concentration of Mg^{2+} or Fe^{3+} and Cl^- need to be modified and calculated. Also, for Pearl® process, caustic soda is added for increasing pH, so the concentration of Na^+ needed to be calculated for each pH.

Step 1. Set the ratio of Mg^{2+} or Fe^{3+} (R) with total phosphorus concentration.

Step 2. Calculated Mg^{2+} or Fe^{3+} and Cl^- concentration with known total phosphorus concentration.

$MgCl_2$ as additional chemical

$$[Mg^{2+}] = R_{Mg-P} * [P] \quad (3.15)$$

$$[Cl^-] = [Cl^-]_{initial} + 2 * ([Mg^{2+}] - [Mg^{2+}]_{initial}) \quad (3.16)$$

$FeCl_3$ as additional chemical

$$[Fe^{3+}] = R_{Fe-P} * [P] \quad (3.17)$$

$$[Cl^-] = [Cl^-]_{initial} + 3 * ([Fe^{3+}] - [Fe^{3+}]_{initial}) \quad (3.18)$$

For the Pearl® process, an extra step calculates Na^+ concentration with each pH

Step E1. Calculated total carbon concentration with the initial concentration of H_2CO_3 , HCO_3^- and CO_3^{2-}

Step E2. Set pH to 9, 10, and 11.

Step E3. Calculated the concentration of H_2CO_3 , HCO_3^- , and CO_3^{2-} under new pH with initial total carbon concentration.

Step E4. Calculated the concentration of H_3PO_4 , $H_2PO_4^-$, HPO_4^{2-} and PO_4^{3-} under new pH with known total phosphorus concentration.

Step E5. Calculated the concentration of Na^+ with charge balance equation.

3.3.3 Calculation for results

Visual MINTEQ gives the results about precipitated solid concentration, partial pressure of dissolved gases in aqueous phase, fraction of components that have precipitated and the concentration of inorganic species in the aqueous phase. Table 4.2 shows the various species or complexes that could result from each primary ion as calculated with Visual MINTEQ.

Table 3.2: Model Component and Related Species

Na^+	K^+	NH_4^+	Ca^{2+}	Mg^{2+}	Fe^{2+}	Fe^{3+}
Na^+	K^+	NH_3	$Ca(NH_3)_2^{2+}$	$Mg(NH_3)_2^{2+}$	$Fe(NH_3)_2^{2+}$	$Fe-(Acetate)^{2+}$
Na_2HPO_4	K_2HPO_4	NH_4^+	Ca^{2+}	Mg^{2+}	$Fe(NH_3)_3^{2+}$	$Fe-(Acetate)^3$
$Na_2PO_4^-$	$K_2PO_4^-$	$NH_4SO_4^-$	$Ca-Acetate^+$	$Mg_2CO_3^{2+}$	$Fe(NH_3)_4^{2+}$	$Fe(OH)_2^+$
Na-Acetate	K-Acetate		$CaCl^+$	Mg-Acetate	$Fe(OH)_2$	$Fe(OH)_3$
NaCl	KCl		$CaCO_3$	$MgCl^+$	$Fe(OH)_3^-$	$Fe(OH)_4^-$
$NaCO_3^-$	KH_2PO_4		$CaH_2PO_4^+$	$MgCO_3$	Fe^{2+}	$Fe(SO_4)_2^-$
NaH_2PO_4	$KHPO_4^-$		$CaHCO_3^+$	$MgHCO_3^+$	Fe-Acetate+	Fe^{3+}
$NaHCO_3$	KOH		$CaHPO_4$	$MgHPO_4$	$FeCl^+$	$Fe_2(OH)_2^{4+}$
$NaHPO_4^-$	KPO_4^{2-}		$CaNH_3^{2+}$	$MgOH^+$	$FeH_2PO_4^+$	$Fe_3(OH)_4^{5+}$
NaOH	KSO_4^-		$CaOH^+$	$MgPO_4^-$	$FeHCO_3^+$	Fe-Acetate ²⁺

NaPO_4^{2-}	CaPO_4^-	MgSO_4	FeHPO_4	FeCl^{2+}
NaSO_4^-	CaSO_4		FeNH_3^{2+}	$\text{FeH}_2\text{PO}_4^{2+}$
			FeOH^+	FeHPO_4^+
			FeSO_4	FeOH^{2+}
				FeSO_4^+

For example, the species related to Ca^{2+} are $\text{Ca}(\text{NH}_3)_2^{2+}$, Ca^{2+} , Ca-Acetate⁺, CaCl^+ , $\text{CaCO}_3(\text{aq})$, $\text{CaH}_2\text{PO}_4^+$, CaHCO_3^+ , $\text{CaHPO}_4(\text{aq})$, CaNH_3^{2+} , CaOH^+ , CaPO_4^- and $\text{CaSO}_4(\text{aq})$. MINTEQA2 uses equilibrium constants, mass balances and charge balances to determine individual concentrations and the fraction of the total.

Total alkalinity was determined using Eq (3.10) which accounts for concentrations of HCO_3^- , CO_3^{2-} , HPO_4^{2-} , PO_4^{3-} and OH^- . In this case alkalinity is the traditional definition of titration to pH=4.5 so PO_4^{3-} represents 2 equivalents of alkalinity since the base form does not get fully converted to the acid form (H_3PO_4) at pH=4.5. The loss of inorganic carbon to the gas phase as $\text{CO}_2(\text{g})$ was determined by subtracting the solid carbonate concentrations and aqueous components from the initial total carbonate concentration.

CHAPTER 4. RESULTS DISCUSSION

The results for the modeling of two P recovery and one P removal methods are provided in this chapter. For each of the methods, the modeled constituent concentrations are provided first followed by precipitation of solids, alkalinity and the fraction of carbon lost. The influence of temperature on the results is explored and finally, the amount of chemical additions is determined for the three scenarios.

4.1 AirPrex

AirPrex is a pre-dewatering P recovery technology that is applied to the digested sludge. The constituent concentration for model work was collected from pilot testing with sludge samples tested each week from June 15 to August 3 in 2016 for a total of eight samples. A summary of digested sludge quality is shown in Table 4.1

Table 4.1: Constituent concentration in digested sludge

Descriptions	Unit	Digested Sludge		
		Maximum	Minimum	Average
pH	-	7.3	7.3	7.3
Alkalinity	mg/L as CaCO ₃	5300	4330	4723
Ca	mg/L	843.7	688.6	780
Mg	mg/L	265.4	156.4	198
Fe	mg/L	518.4	426.1	464
K	mg/L	337.7	307.8	322
Na	mg/L	150.7	129.6	139
TP	mg/L	1104.3	849.6	981

NH ₄ ⁺	mg/L	1660	1520	1593
CH ₃ COOH	mg/L			670

Converting units from mg/L to mol/L, the concentration of Mg is 0.00815 mol/L, PO₄-P is 0.03165 and NH₄-N is 0.0885 and the molar ratio of Mg: PO₄:NH₄ is approximately 1: 4: 11. From literature review, phosphorus can be recovered as struvite when the molar ratio is near 1:1:1 for Mg, PO₄ and NH₄ and therefore magnesium is the limiting chemical for precipitation.

For the AirPrex model, magnesium chloride was added to the digested sludge and the equilibrium components concentration with different magnesium concentrations were determined. From literature review, the key cations which have direct influence on struvite precipitation and phosphorus recovery are magnesium and calcium. Virtual Minteq gave the percentage of component precipitation and the species concentration in the aqueous phase. Figures 4.1 and 4.2 below show the relative concentrations of calcium and phosphorus in solution and solid phases. The left axis in figure 4.1 indicates the ratio of equilibrium concentration with initial influent concentration and the right axis indicates the percentage of precipitation. Figure 4.2 provides information of solid concentration produced in the AirPrex process.

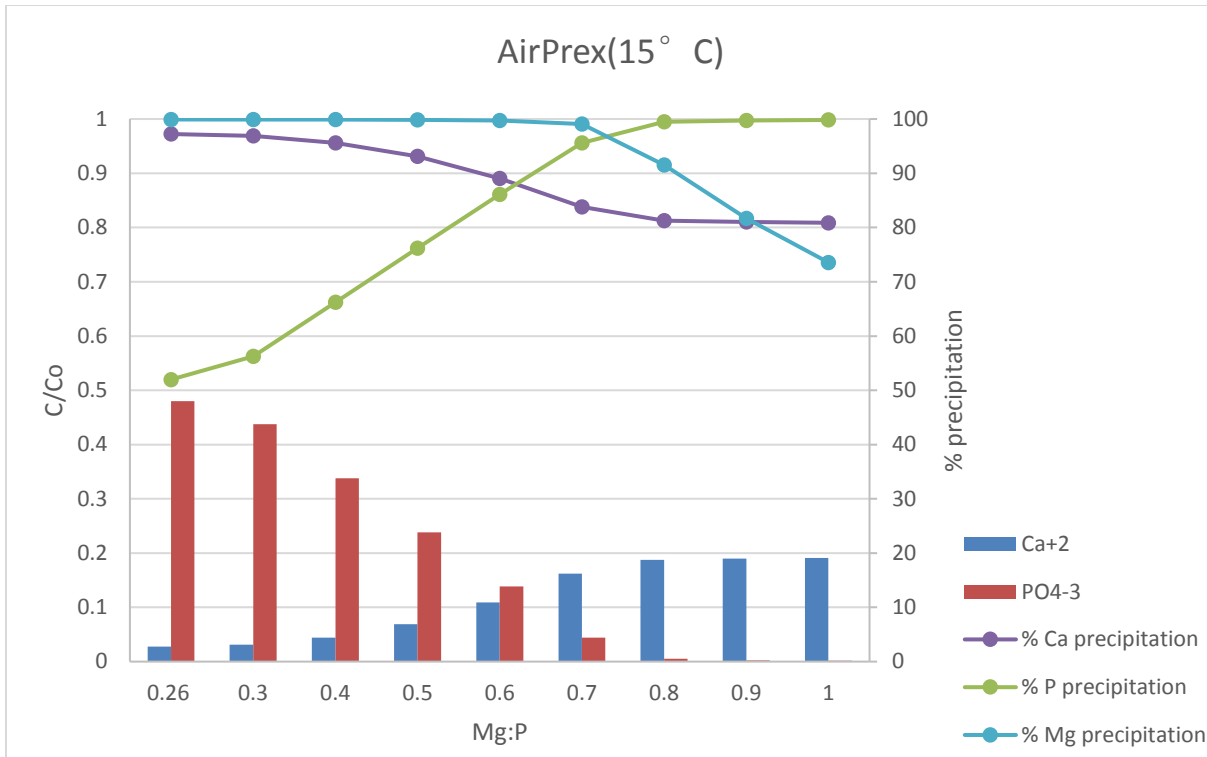


Figure 4.1: The ratio of equilibrium concentration in solution with initial concentration and precipitation (%) with various Mg:P ratios for significant ions in the AirPrex Process at 15°C

Figure 4.1 shows, with Mg increasing, the percentage of calcium precipitation decreases slowly and the percentage of phosphorus precipitation increases. On the other hand, in the aqueous phase, the calcium concentration increases and phosphate decreases as the magnesium concentration increases.

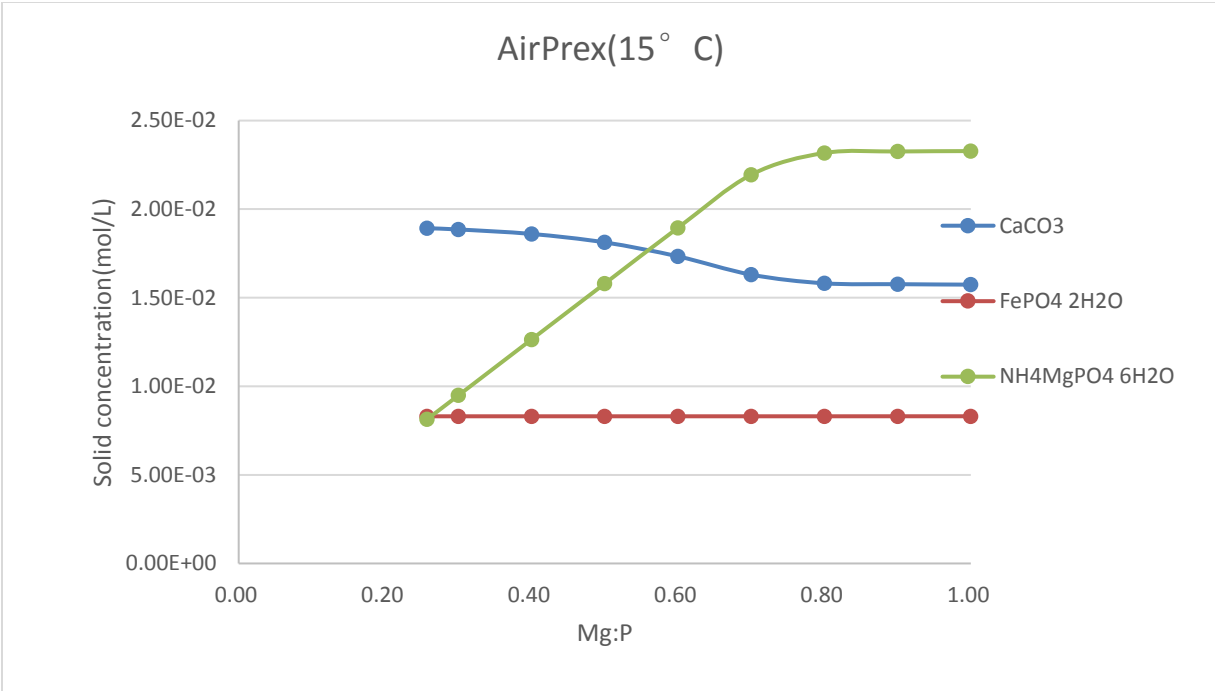


Figure 4.2: Produced solid concentration in Airprex Process at 15°C

From figure 4.2, there are three solids produced in the process; calcite (CaCO_3), strengite ($\text{FePO}_4 \cdot 2\text{H}_2\text{O}$) and struvite ($\text{NH}_4\text{MgPO}_3 \cdot 6\text{H}_2\text{O}$). The amount of strengite precipitation is almost constant with various magnesium concentrations which is about $8.3 \times 10^{-3} \text{ mol/L}$. Ferric concentration in the water source is $8.3 \times 10^{-3} \text{ mol/L}$, so nearly 100% of ferric is precipitated. With Mg concentration increasing, the amount of produced calcite decreases affecting the amount of calcium in water.

Additionally, Figure 4.2 shows that struvite precipitation keeps increasing with additional magnesium addition when $\text{Mg:P} < 0.7$ although it stabilizes above this ratio. With the ratio of Mg and P increase 0.1, there are $3.16 \times 10^{-3} \text{ mol/L}$ struvite could be produced. In this water sample, increase 0.1 ratio of Mg and P is same with add $3.16 \times 10^{-3} \text{ mol/L}$ magnesium chloride. So when $\text{Mg:P} < 0.7$, all of additional magnesium is used for struvite synthesis. When Mg:P reaches 0.7, the rate of additional precipitation decreases rapidly. From Figure 4.1, Mg precipitation percent

decreases from 100% meaning that there is surplus magnesium which could not precipitate and the usage rate of additional magnesium chloride is keeping decrease from $Mg:P = 0.7$. At the point where $Mg:P$ is 0.8, the amount of struvite produce reach optimal which about $2.33 \times 10^{-2} \text{ mol/L}$ and the percentage of phosphorus recovered reaches 99%.

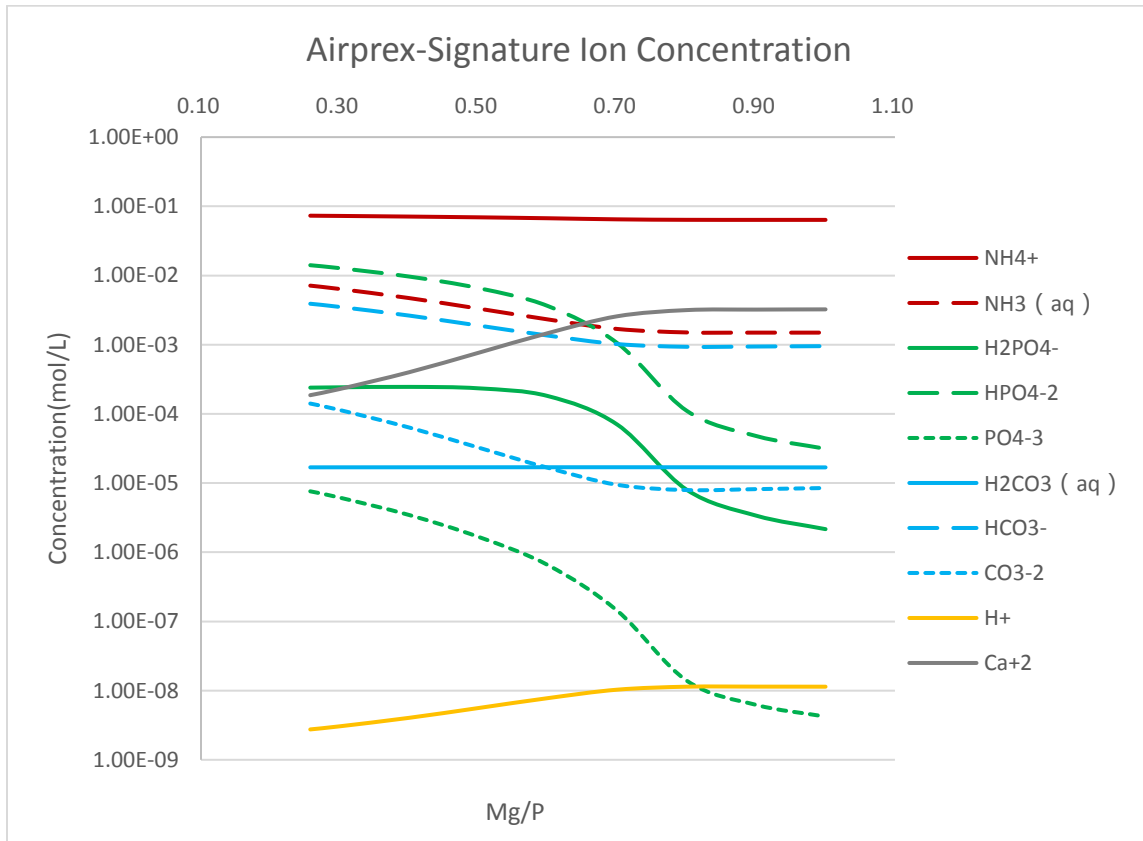


Figure 4.3: Signature Ion Concentration in Chemical Equilibrium for AirPrex

Figure 4.3 shows the concentration of significant ions related to the solids precipitation. From Figure 4.3, there are five groups of ions which are ammonium/ammonia, dihydrogen phosphate/ hydrogen phosphate/ phosphate, carbonic acid/ bicarbonate/ carbonate, hydrogen and calcium. With Mg concentration increasing, more and more phosphate is precipitated as struvite. At the same time, hydrogen phosphate and dihydrogen phosphate dissociate to release more phosphate and hydrogen. So in the process, hydrogen concentration increase with Mg addition resulting in a

pH. Because the partial pressure of CO₂ is fixed, the concentration of H₂CO₃ keeps constant. While with pH decrease, HCO₃⁻ and CO₃²⁻ tend to form H₂CO₃ and more carbon is lost to the gas phase. Under this situation, with increased Mg concentration, more inorganic carbon is released as CO₂ and less calcite is produced.

Table 4.2 gives the information at point Mg:P=0.8 with different temperatures. It includes the percentage of phosphorus removal, percentage of carbon loss and alkalinity at chemical equilibrium with three temperatures; 15°C, 25°C and 35°C.

Table 4.2: AirPrex Parameter Sensitivity at Mg/P=0.8 for different temperatures.

Temperature	15°C	25°C	35°C
% P precipitation	99.48	99.45	99.38
% C loss	81.09	81.28	81.44
Alkalinity as CaCO ₃ (mg/L)	54.36	43.18	34.76

From this table, it is clear that temperature does not impact the process output significantly.

For carbon loss, there are two reasons; precipitation as calcite and loss as CO₂ to the atmosphere.

Visual MINTEQ gives the concentration of inorganic species in aqueous and the concentration of solid produced. With the initial total carbon, the amount of carbon loss as gas phase could be calculated with the law of mass conservation.

Figure 4.4 gives the percentage of carbon lost with various Mg/P ratios.

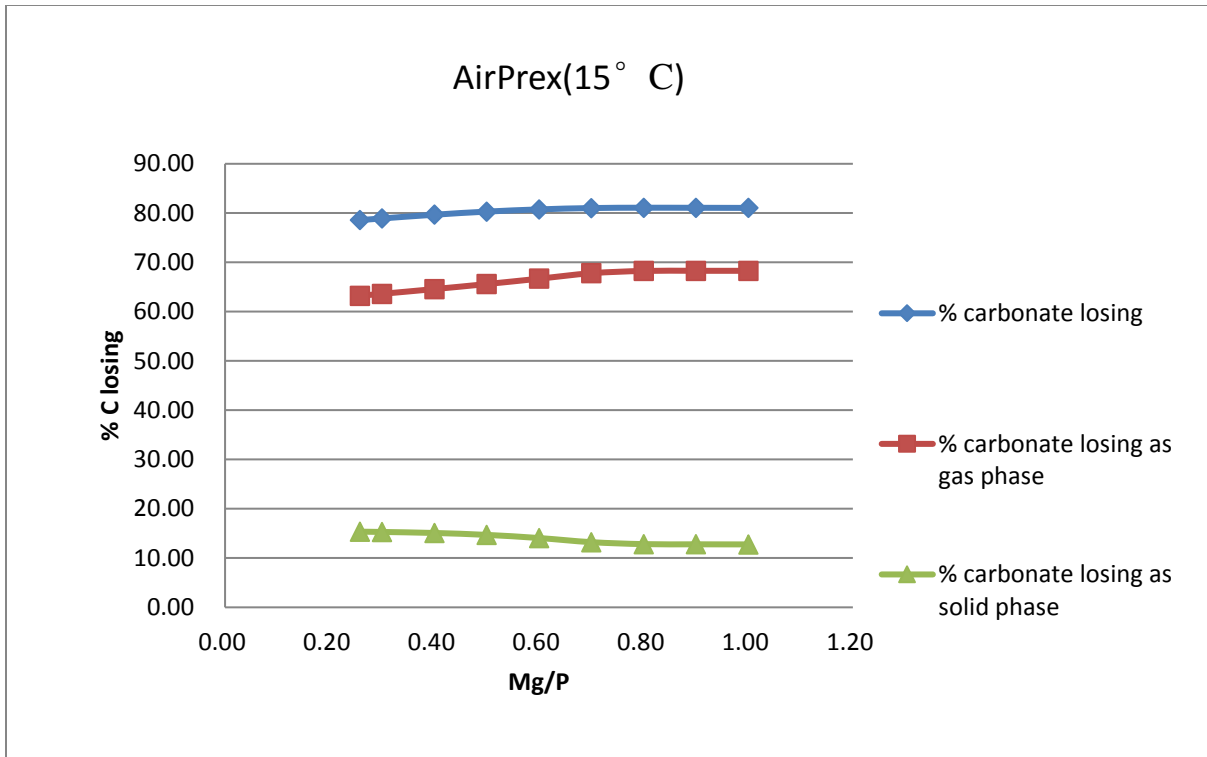


Figure 4.4: Carbonate losing in Airprex Process at 15°C

The results in Figure 4.4 indicate that over 65% of the inorganic carbon is lost in the gas phase with the rest being precipitated as calcite. Because P recovery processes involve aeration, the oversaturated carbonic acid is lost to the gas phase with the fixed CO₂ partial pressure.

Figure 4.5 shows the alkalinity as CaCO₃ at three temperatures with various Mg/P ratios for the AirPrex technology.

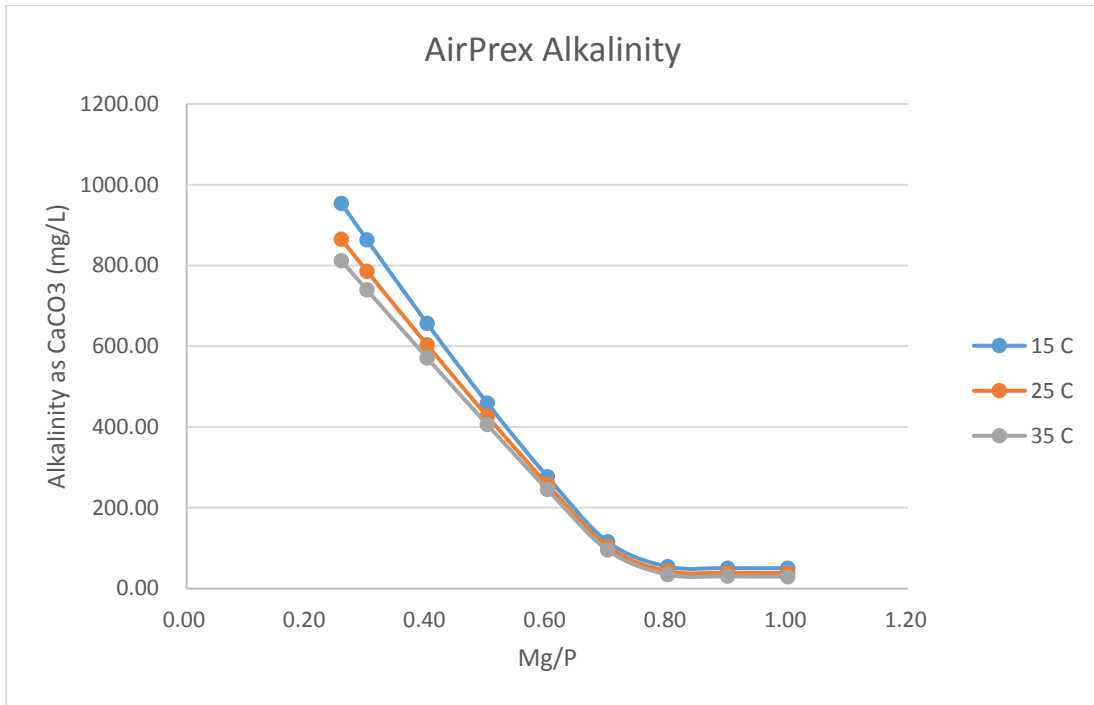


Figure 4.5: Alkalinity in 15°C 25°C and 35°C in Airprex Process

As shown in figure 4.5, at equilibrium, alkalinity decreases when the Mg/P ratio increases. Alkalinity is related to carbonate, bicarbonate, hydrogen phosphate, phosphate and hydroxide and the decrease as Mg concentration increases is due to additional struvite precipitation and more phosphorus removal. pH decrease in the process because with phosphorus removal, hydrogen phosphate and dihydrogen phosphate dissociated with pH decrease, more and more H₂CO₃ formed and more carbon lost as CO₂ with the decrease of HPO₄⁻, PO₄⁻, CO₃²⁻ and HCO₃⁻. At the same Mg/P ratio, the alkalinity is lower when temperature is higher.

4.2 Pearl® Process

The Ostara Pearl® nutrient recovery process is a sludge post-dewatering P recovery technology. Compared with the AirPrex process, the influent water needs to pass through a dewatering process such as centrifugation. The centrate from the centrifuge process is the influent of the Pearl® process. For the modeling discussed here, centrate samples were collected from pilot testing using MWRD sludge each week from April 5 to July 31 in 2016 for a total of eighteen samples. A summary of centrate quality is shown in Table 4.3

Table 4.3: Water quality of centrate used in model

Descriptions	Unit	Centrate		
		Maximum	Minimum	Average
pH	-	8.3	7.8	8.0
Alkalinity	mg/L as CaCO ₃	3860	1190	3000
Ca	mg/L	65	32	44
Mg	mg/L	11.7	5.2	7.9
Fe	mg/L	12.1	0.5	4.1
K	mg/L	301	224	266
Na	mg/L	145	113	136
TP	mg/L	305	206	236
NH ₄ ⁺	mg/L	1280	783	1176
CH ₃ COOH	mg/L			110

When comparing the quality of digested sludge and centrate through the dewatering process, much of phosphorus and metals ions are removed with the solids in the dewatering process. The

concentration of magnesium decreases significantly from 265 mg/L to 11 mg/L and the concentration of phosphorus decreases from 1104 mg/L to 305 mg/L. The ratio of Mg and P change from 1:11 to 1:23 so magnesium needs to be added to assure adequate precipitation of phosphorus as struvite. However, the available phosphorus in centrate is much lower than it is in digested sludge but so is the magnesium. Therefore, for the Ostara process, magnesium in the form of magnesium chloride needs to be added and since the reaction occurs faster at higher pH values, sodium hydroxide is also added. For the Pearl® process, the modeling exercise was divided into two steps (1) modifying the ratio of Mg and P with a fixed pH similar to the AirPrex analysis and (2) repeating step one with different pH values.

4.2.1. Pearl® Process Model with pH=8

Figures 4.6 and 4.7 show the results of significant ion concentrations in solution and information about the precipitation of solid at pH=8. In this model, the ratio of magnesium and phosphorus were modified from 0.3 to 1.2 in order to find the optimal point for P removal.

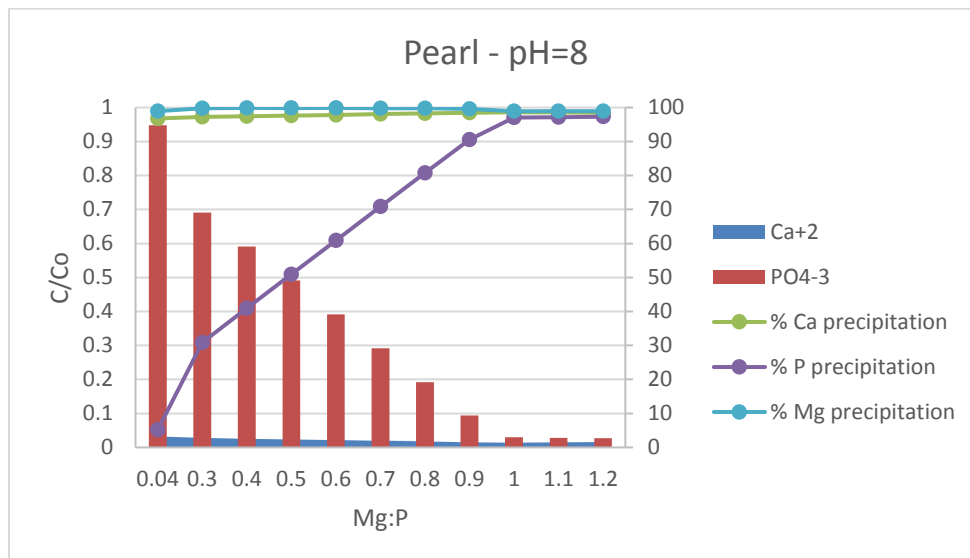


Figure 4.6: The ratio of equilibrium concentration in solution with initial concentration and precipitation (%) with various Mg and P ratios for significant ions in the Pearl® process at 15°C

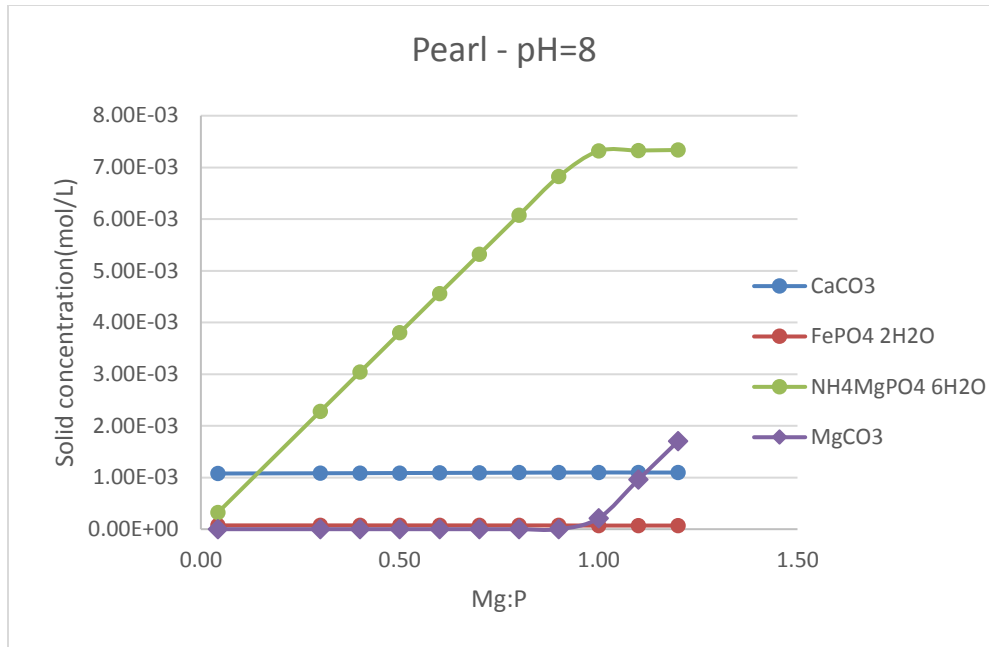


Figure 4.7: Produced solid concentration in Pearl® Process at 15°C

From figure 4.7, there are four solids produced which are calcite (CaCO_3), strengite ($\text{FePO}_4 \cdot 2\text{H}_2\text{O}$), struvite ($\text{NH}_4\text{MgPO}_4 \cdot 6\text{H}_2\text{O}$) and magnesite (MgCO_3). The amount of strengite and calcite are relatively constant with varying magnesium concentrations. The amount of strengite is low at about 7.3×10^{-5} mol/L. However, from figure 4.6, about 99% iron precipitated as strengite at equilibrium but since the initial ferric concentration is very low which is 4.1 mg/L , there is only a small amount of strengite. The initial calcium concentration was 421 mg/L and as Figure 4.6 shows, at chemical equilibrium, the percent of precipitation varies slightly with increases about 2% with Mg/P in the range of 0.04 to 1.2 and it is also close to 98% removal.

Struvite precipitation increases with greater magnesium concentrations. It increases from 3.2×10^{-4} to 7.3×10^{-3} molar per liter when Mg/P increases from 0.04 to 1. In figure 4.6, when Mg/P=1.0, phosphorus precipitation reaches the optimal point which is about 97% removal and is constant with Mg/P increasing. It is because struvite precipitation stays at a maximum value from the ratio of Mg/P=1.0. In addition, from figure 4.7, magnesite appears from this point and increases with

more magnesium added. So when Mg/P is smaller than 1.0, almost all of magnesium added in uses for struvite producing. From Mg/P equal and greater than one, some extra magnesium is precipitated as magnesite.

Table 4.4 gives the information at the ratio Mg:P=1.0 with different temperatures for the Pearl® process. It includes the percentage of phosphorus removal, percentage of carbon loss and alkalinity at chemical equilibrium with three temperatures; 15°C, 25°C and 35°C.

Table 4.4: Important information at Mg/P=1.0 with different temperature for Pearl® (pH=8)

Temperature	15°C	25°C	35°C
% P precipitation	97.02	98.09	98.09
% C loss	61.47	71.53	79.89
Alkalinity as CaCO ₃ (mg/L)	1071.62	737.28	458.43

From table 4.4, it is clear that the temperature effect on P precipitation is minimal. However, the percent of carbon loss increases as temperature increases and alkalinity at chemical equilibrium decreases as temperature increases. This is due to the solubility of carbon dioxide in water decreasing as the temperature increases. In the model, the partial pressure of CO₂ is fixed, but the Henry's law constant changes with temperature and at the optimal point where Mg/P=1.0, there is a little MgCO₃ precipitation.

Figures 4.8 and 4.9 shows the carbon loss and alkalinity with various Mg/P ratios at pH=8 for the Pearl® process.

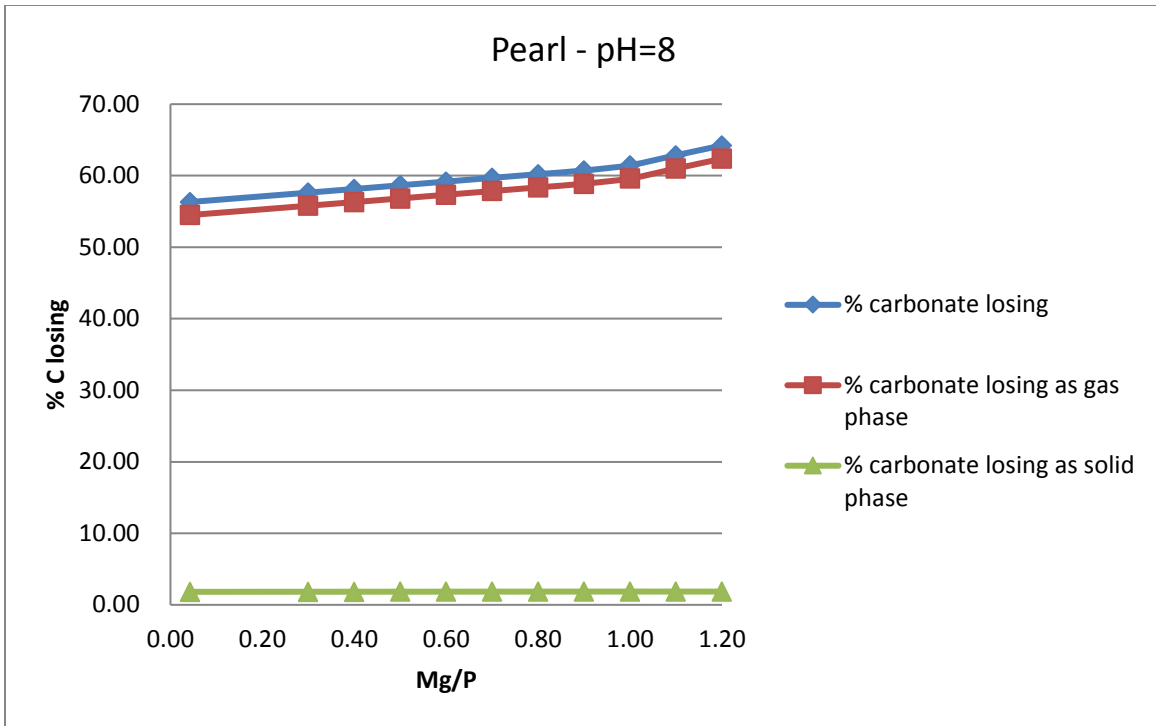


Figure 4.8: Carbon Loss for Pearl® Process at pH=8 and 15°C

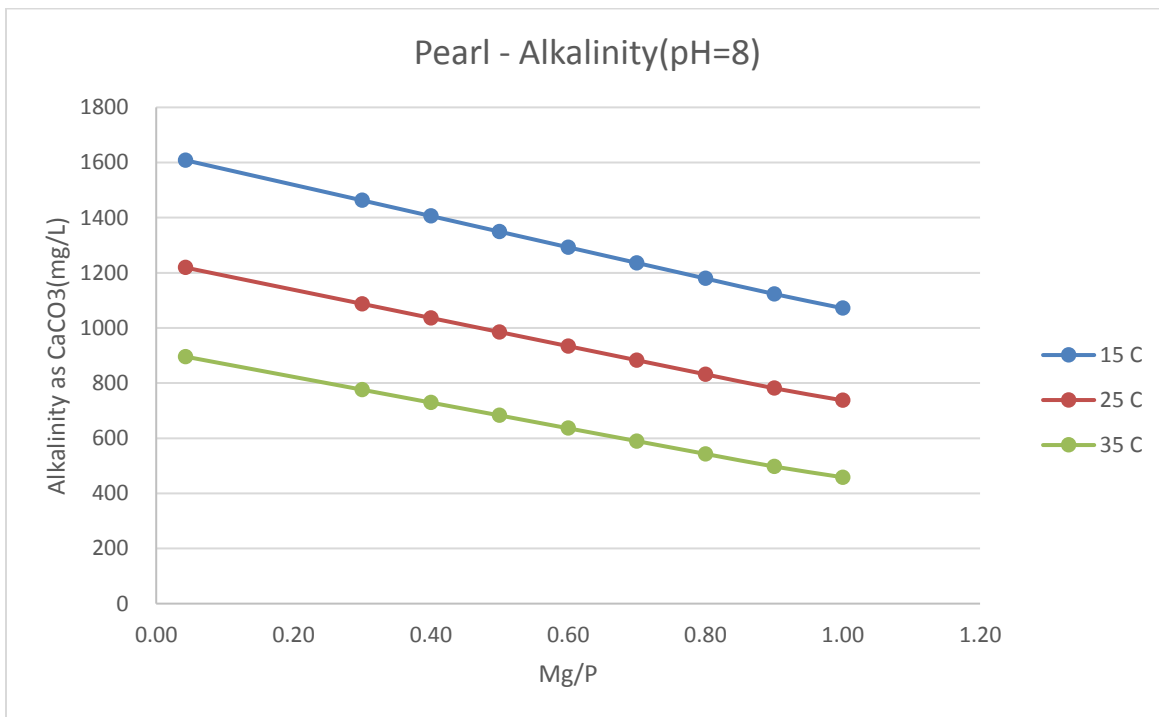


Figure 4.9: Alkalinity in 15°C 25°C and 35°C in Airprex Process

Figure 4.8 shows that carbonate losses increase with Mg/P ratio increase and the most of carbon loss is to CO₂ in the gas phase with only a small fraction precipitating as calcite because the available calcium is low (0.0011 mol/L). From model results, about 2% of the inorganic carbon is lost as solid. Also shown in figure 4.9, as the Mg/P ratio increases, alkalinity decreases and with a fixed Mg/P, alkalinity decreases as temperature increases. This happens because when Mg increases, struvite precipitation increases which reduces phosphate in the aqueous phase and in addition, temperature reduced the solubility of CO₂ which elevates the carbon loss to the gas phase.

4.2.2. Pearl® Process Model with various pH

In order to adjust pH, NaOH needs to be added. Besides the initial pH=8, 3 additional conditions were modeled: pH=9, pH=10 and pH=11. Figure 4.10 shows the ratio of equilibrium concentration in solution with the initial total concentration for calcium and phosphorus with varying Mg/P ratios and under different pH values. The right axis indicates the ratio for phosphorus and the left axis indicates the ratio for calcium. Figure 4.11 shows the amount of four precipitated solids with various Mg/P ratios and different pH values.

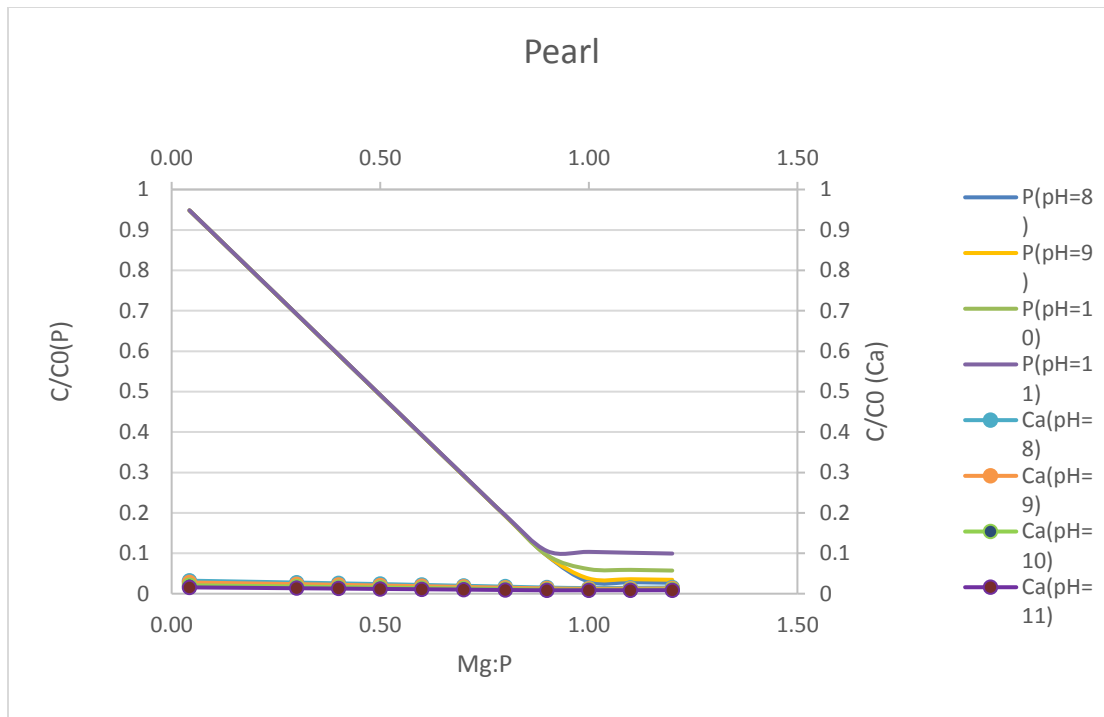
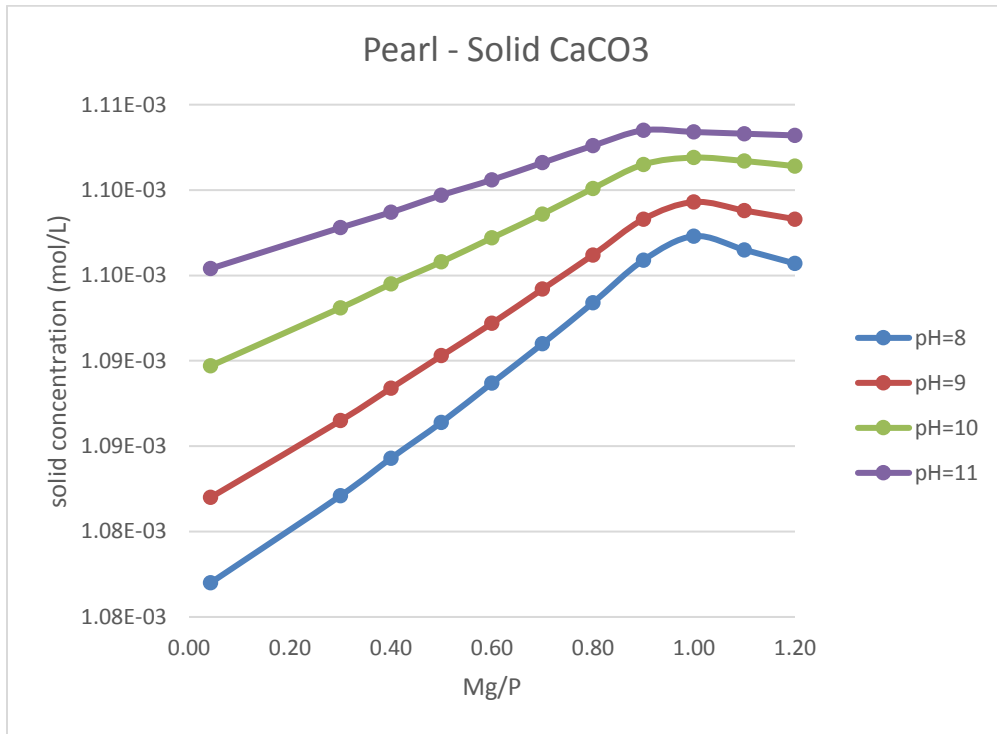


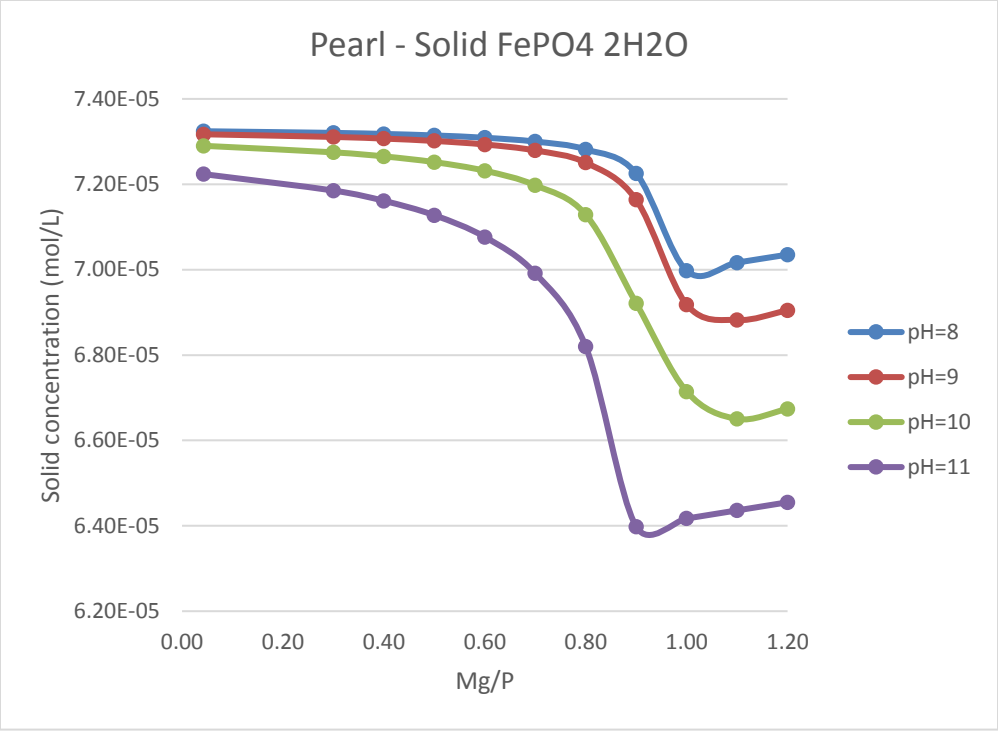
Figure 4.10: The ratio of equilibrium concentration in solution and initial concentration for Ca^{2+} and PO_4^{3-} with various Mg and P ratio under different pH in Pearl® Process

In Figure 4.10, the calcium concentration is nearly constant as magnesium concentration increases and pH values increase. Phosphorus concentration decreases as the magnesium concentration increases and with pH decrease in high magnesium concentrations. At high magnesium concentrations, MgCO_3 is produced and when caustic soda is added, carbonic acid is a weak acid that dissociates to produce HCO_3^- and CO_3^{2-} , increasing MgCO_3 precipitation and the available Mg for struvite precipitation is limited. pH appears to affect the optimal P removal level and higher pH response to higher optimal P concentration. When $\text{Mg/P} < 0.8$, the P concentration is same with different pH and decreases with a stable rate. In the range $0.8 < \text{Mg/P} < 1.0$, with over supply Mg precipitated as MgCO_3 , P concentration transfer to each optimal level. pH at 8 is could reach the least P concentration in this model work which is under initial aqueous concentration because with increasing pH, CO_3^{2-} tends to form. Under this condition,

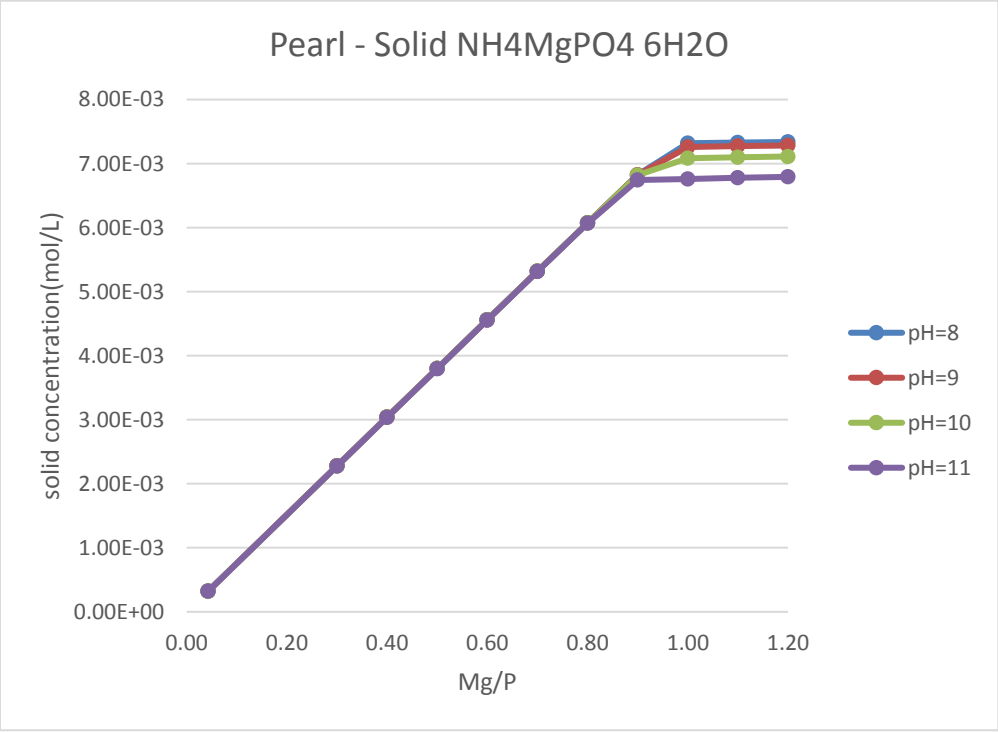
compared with pH=8, more Mg produce as solid $MgCO_3$ at pH=11. In the other word, compared with pH =8, less Mg is produced as struvite which precipitated while consuming phosphorus at pH=11.



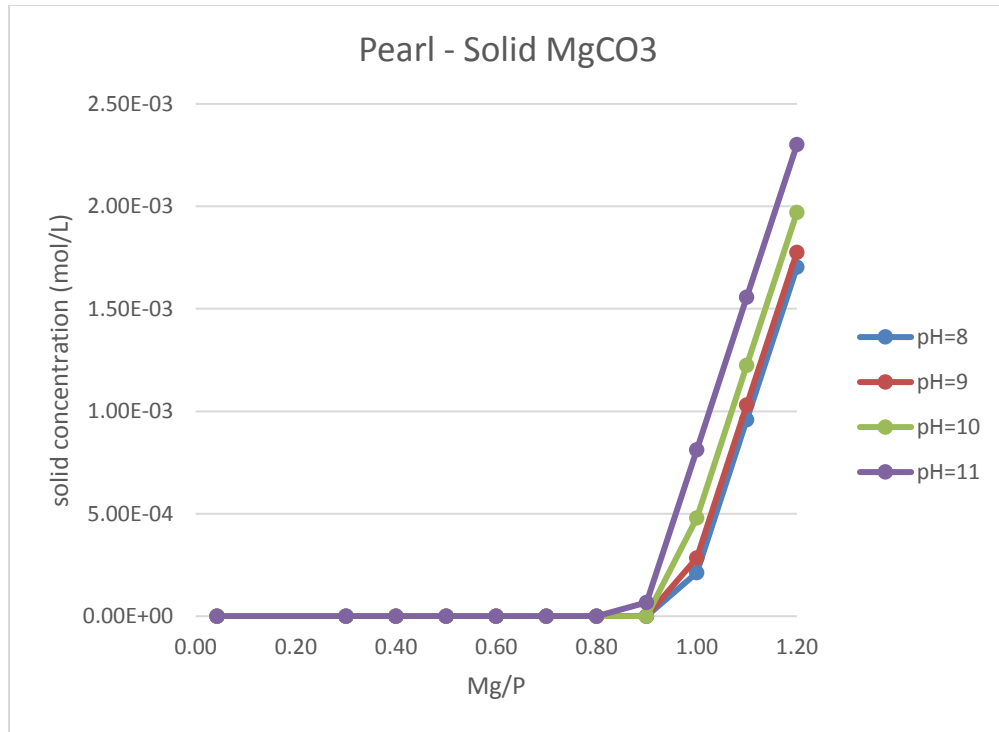
(a)



(b)



(c)



(d)

Figure 4.11: Four solid precipitation concentration with various Mg/P and different pH. (a) Calcite precipitated concentration. (b) Strengite precipitated concentration. (c) Struvite precipitated concentration. (d) Magnesite precipitated concentration

Figure 4.11, in the range $Mg/P < 0.8$, calcite precipitation improved with Mg/P increasing and pH increasing, and strengite precipitation slightly reduced with Mg/P increasing and pH increasing, and struvite precipitation is increasing with Mg/P increasing and without pH effect. In this range, magnesite is not produced. In the range, $0.8 < Mg/P < 1.0$, the precipitation situations for all four solids are changed. Calcite precipitation transfers to constant or has slight decreasing with Mg/P increasing. pH increasing still improve calcite precipitation. Strengite precipitation jumped in the transfer range and pH increasing still reduced precipitation. Struvite transfer to constant in the range and the effect of pH could be found. pH increasing reduces struvite precipitation. So for P removal and struvite precipitation, pH=8 is the optimal. Now, magnesite start produced and will increases rapidly with Mg/P increasing, and the precipitation increases with pH increasing.

For alkalinity and carbon loss, pH is one of the most important conditions. From Figure 4.11(a) and (d), the amount of carbon precipitation is affected by pH, but only a small fraction of carbon precipitates. Figure 4.8 also shows that when pH=8, only about 2% carbon is lost as the solid phase. Figures 4.12 and 4.13 shows the C loss and alkalinity as CaCO₃ for Pearl® under different pH values.

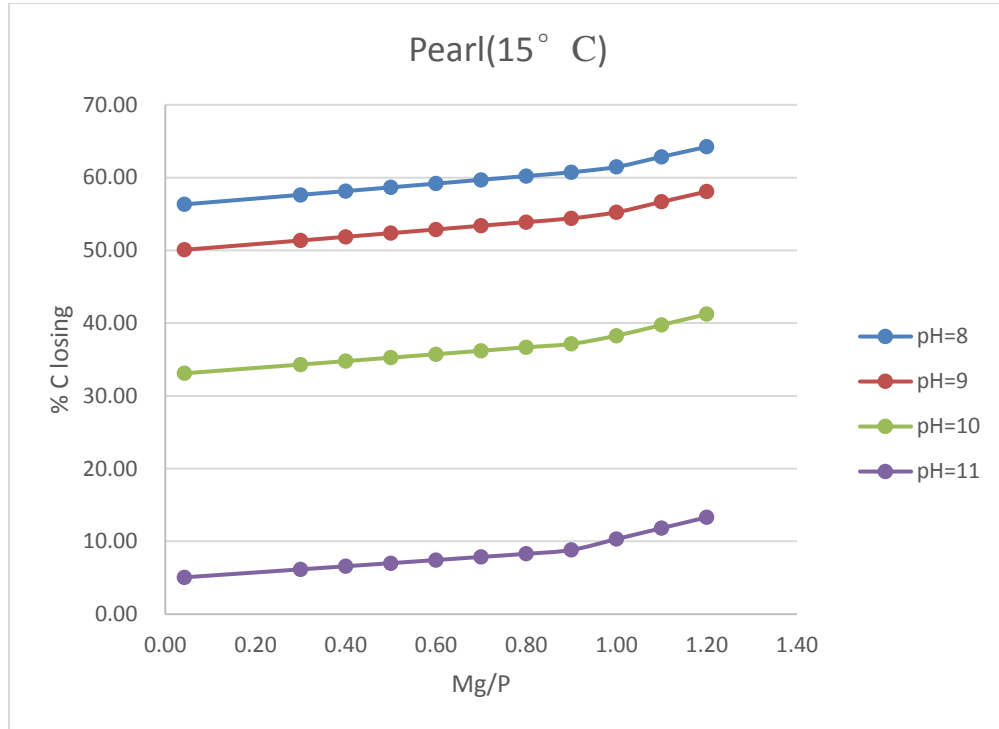


Figure 4.12: C loss with different pH values for the Pearl® process.

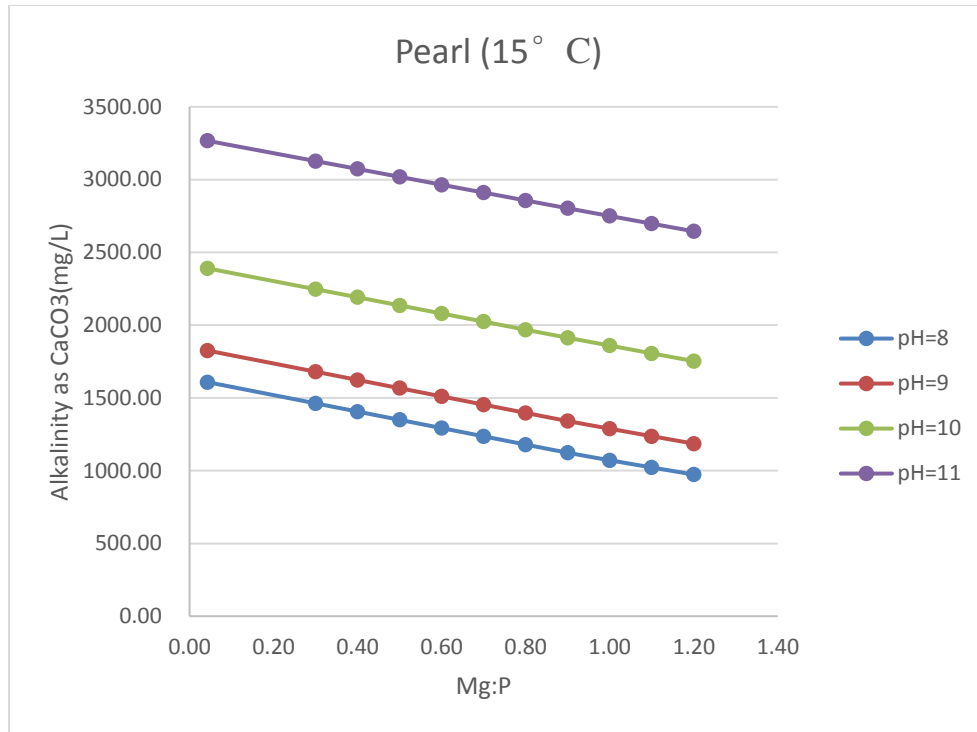


Figure 4.13: Alkalinity as CaCO₃ with different pH values for the Pearl® process

From these figures, when pH increases, C losses decrease and alkalinity increases. This is because with pH increasing, less HCO₃⁻ transfers to H₂CO₃(aq) and more HCO₃⁻ transfers to CO₃²⁻. So carbon lost as gas phase is decreased. It is showed in the results that of the total carbon loss, over 90% carbon is lost to the gas phase. At the same time, with CO₃²⁻ concentration increasing, alkalinity increases.

4.3 Ferric Chloride Addition

This method removes phosphorus using ferric chloride with the influent being digested sludge. The data shown in Table 4.1 was used in this modeling exercise. Ferric chloride is added for the precipitation of ferric phosphate and therefore the ratio of Fe to P was varied to understand the impact on P removal. Figures 4.14 and 4.15 gives the information about the percentage of the significant ions and the amount of the precipitated solid.

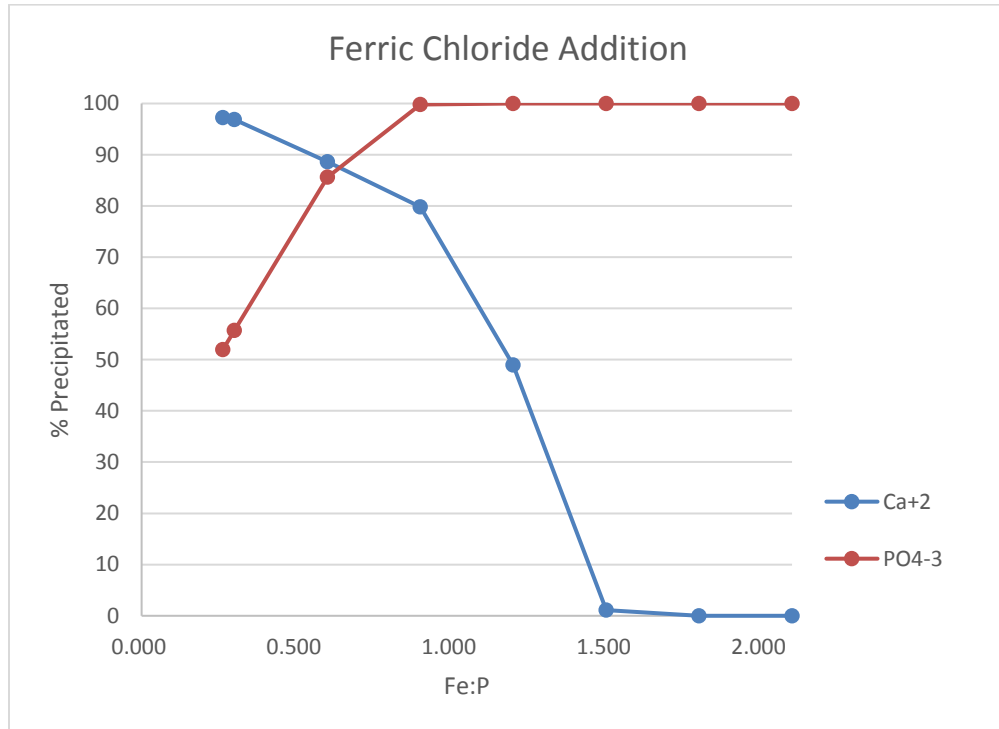


Figure 4.14: Calcium and phosphorus precipitation (%) in removal method with ferric chloride

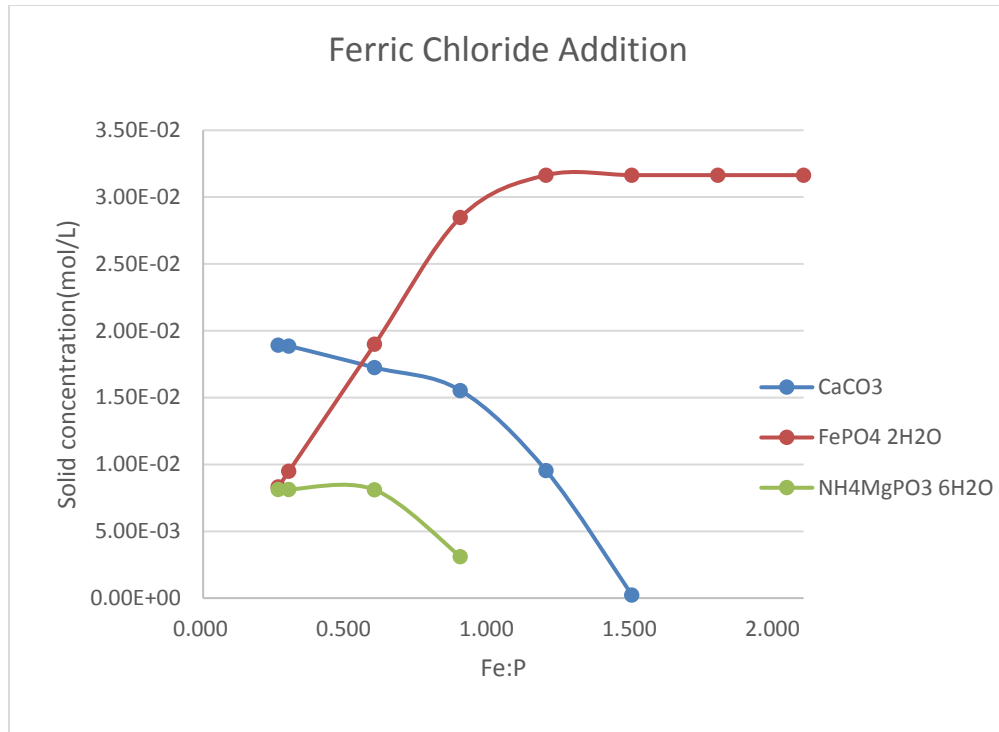


Figure 4.15: The amount of precipitated solid in removal method with ferric chloride

Figure 4.15 gives the information about the solids that are precipitated. There are three solids produced in the process; calcite, strengite and struvite. The amount of struvite produced decreases as Fe/P increases and becomes negligible when Fe/P=1.0. With the Fe concentration increase, more and more strengite is produced until most of the phosphorus is precipitated. From Figure 4.14, at the point Fe/P=1.2, almost 100% of phosphorus is removed as strengite. For the last solid, calcite precipitation decreases with Fe/P increase and disappears at Fe/P is greater than 1.5 because approximately 80% of the carbonate is removed to the gas phase.

Figures 4.16 and 4.17 gives show the about fraction of carbon loss and equilibrium alkalinity for the process over a range of Fe/P ratios.

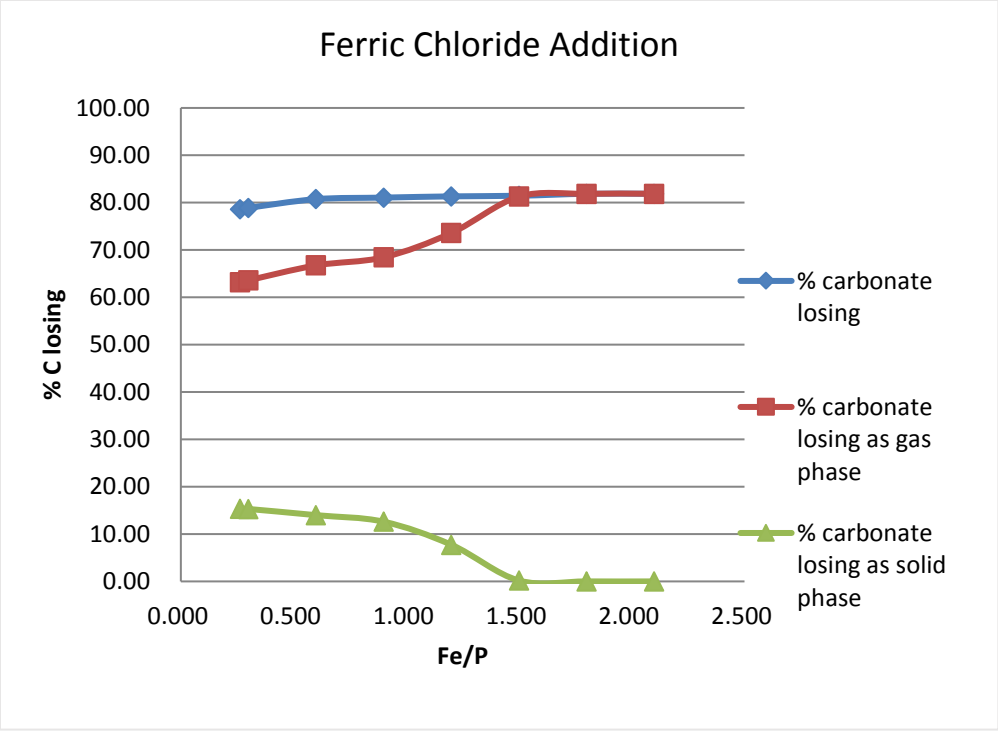


Figure 4.16: C loss for ferric chloride additional method

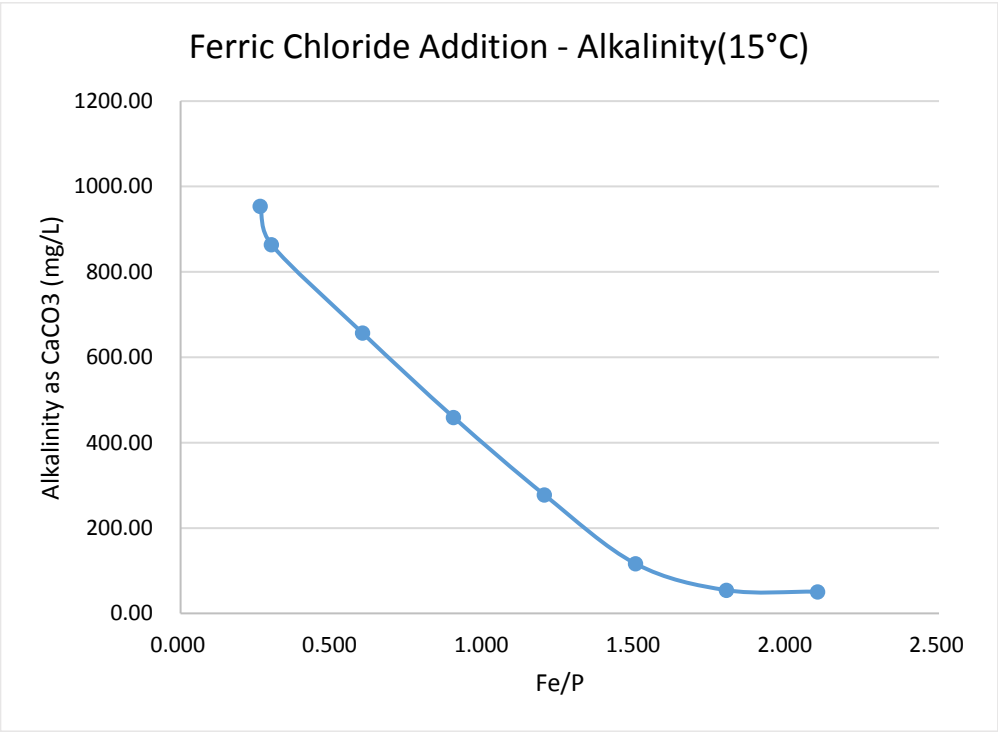


Figure 4.17: Alkalinity as CaCO₃ (mg/L) for ferric chloride additional method

From Figure 4.16, about 80% of the inorganic carbon is lost. When $Fe/P < 1.5$, there are two phases of loss, solid and gas. When $Fe/P > 1.5$, there is not calcite precipitation and other minerals precipitation related to carbon. So all the carbon is lost as gas phase. Regarding alkalinity, Figures 4.14 and 4.15, show that phosphorus precipitates as strengite and reaches about 100% removal when the ratio of ferric and phosphorus is equal to 1.5. So, when $Fe/P < 1.5$, the alkalinity decreases rapidly and when $Fe/P > 1.5$, from Figure 4.17, alkalinity is less than 100.

4.4 Comparison of Three P Recovery/Removal Methods

4.4.1 Amount of phosphorus recovery analysis

For AirPrex and ferric precipitation, the inflow is digested sludge while the inflow for the Ostara Pearl® process is centrate after the dewatering process. From the pilot testing for the two P recovery methods, the inflow rate of Airprex is 3000L/hr and the inflow rate of Pearl® is 0.58 GPM which is equal to 131L/hr. Figure 4.18 below shows the flow scheme with flow rate.

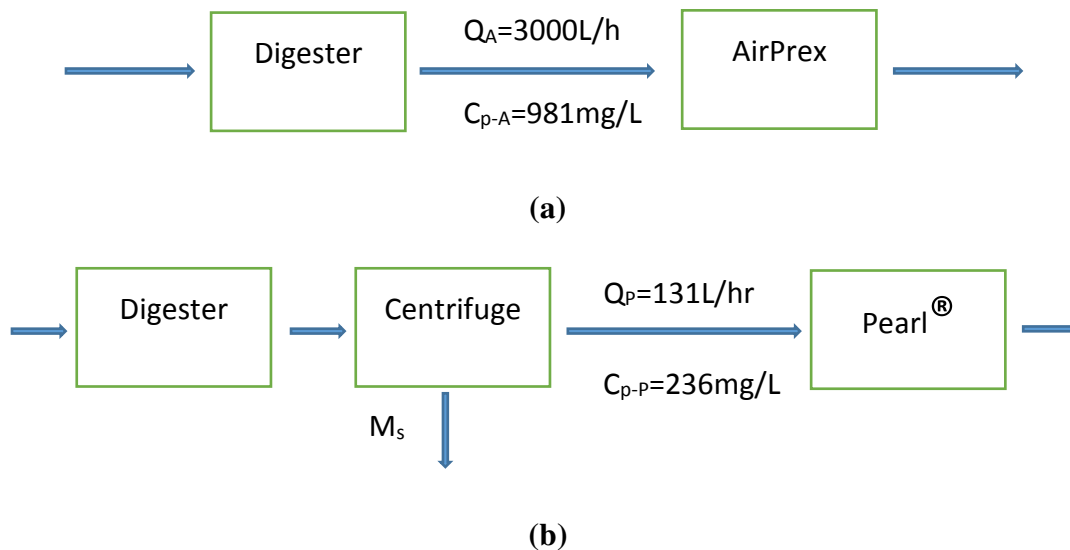


Figure 4.18: Flow rates for AirPrex and Pearl® inflow (a) AirPrex (b) Pearl®

In Figure 4.18(a), Q_A is the inflow rate of AirPrex and C_{p-A} is concentration of total phosphorus in inflow of AirPrex process. In Figure 4.18(b), Q_p is inflow rate of Pearl® and C_{p-P} is total

phosphorus concentration of centrate. M_s is amount of phosphorus per hour for solid sludge. The treatment scale for two pilot testing is same. So, it could be the estimate that the effluence of digester is 3000L/hr for the process with Pearl®.

Depend on the phosphorus mass balance.

$$Q_A \times C_{p-A} = Q_P \times C_{p-P} + M_s \quad (4.1)$$

This means the phosphorus in digested sludge is equal to the sum of phosphorus in centrate and in solid sludge.

Total phosphorus in digested sludge per hour (M_A) is

$$M_A = Q_A \times C_{p-A} = 3000 \times 981 = 2943000 \text{ (mg/hr)} \quad (4.2)$$

Total phosphorus in centrate per hour (M_P) is

$$M_P = Q_P \times C_{p-P} = 131 \times 236 = 30916 \text{ (mg/hr)} \quad (4.3)$$

Total phosphorus in solid sludge

$$M_s = M_A - M_p = 2943000 - 30916 = 2912084 \text{ (mg/hr)} \quad (4.4)$$

So, the available recovery phosphorus for AirPrex and additional method with ferric chloride is 2,943,000 mg/hr and the available recovery phosphorus for Pearl® is 30916 mg/L.

Comparing the amount of phosphorus recovery with the total phosphorus in the initial inflow waste activated sludge, the real P recovery ability for two sludge treatment processes could be determined.

Table 4.5 below give the summary information about optimal P recovery.

Table 4.5: Optimal P recovery information for three methods

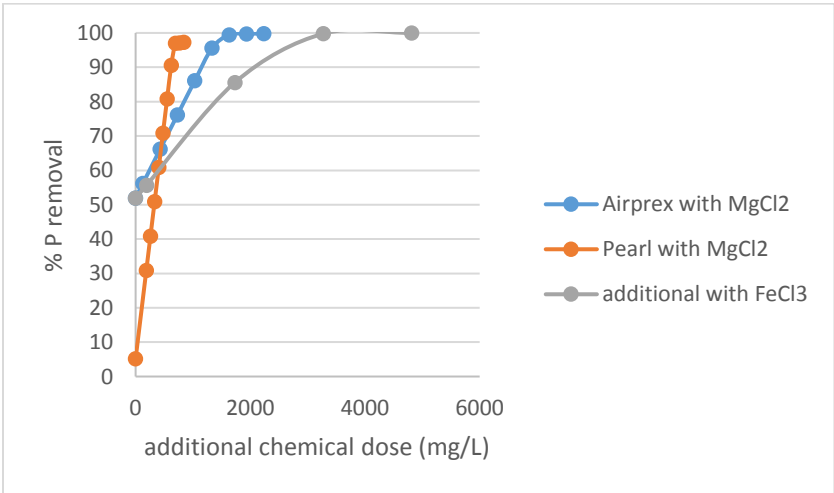
	Method I	Method II	Method III
P recovery technology	AirPrex	Pearl®	FeCl ₃
Optimal %P removal	99.5%	97%	100%

Mg/P or Fe/P at optimal point	0.8	1.0	1.2
The amount of available recovery P(mg/L)	981	236	981
The amount of P recovery at optimal point(mg/hr)	2928000	29868	2943000
Real % P recovery for whole process at optimal point	99.5%	1.01%	100%

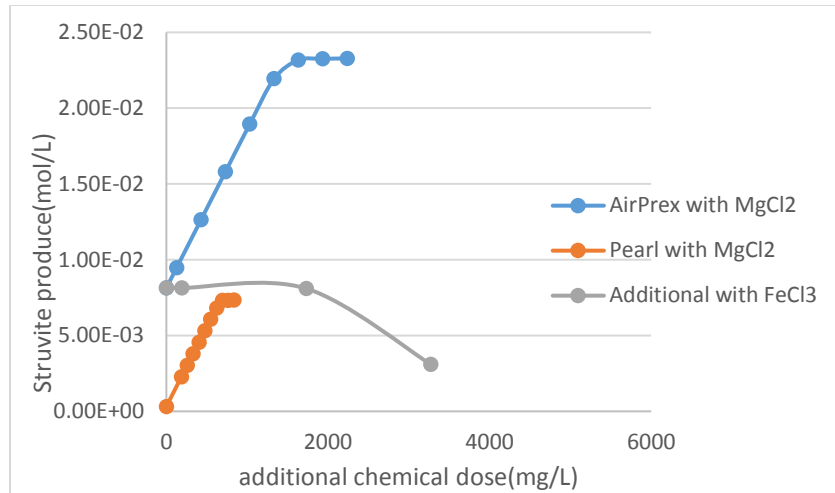
From this table, for pearl® process, 99% phosphorus is removal with solid sludge. Pearl® process reduce the problem of high concentration P reload to wastewater treatment. But compared with Airprex, it does not work well on reducing the phosphorus from the solid sludge stream. So for solid management and disposal, there is a greater challenge for the Pearl® process compared with AirPrex.

4.4.2 Additional chemical dose for three methods

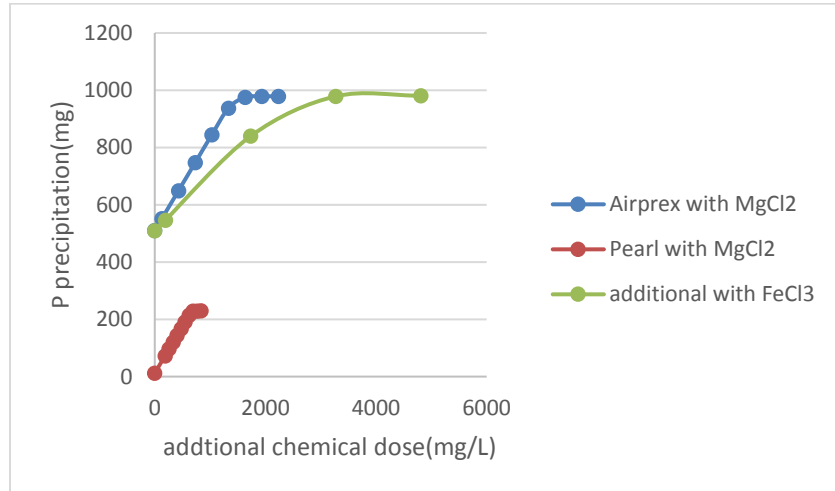
Figure 4.19 shows the additional chemical dose for the three methods. AirPrex only requires one additional chemical MgCl₂. Pearl® process uses two chemicals, MgCl₂ and NaOH, but the optimal pH is near pH = 8 so minimal base will be needed if the stream is near this pH. Figure 4.19 gives the MgCl₂ dose for the Airprex and Pearl® processes, and FeCl₃ dose for the precipitation method.



(a)



(b)



(c)

Figure 4.19: Additional chemical dose for three P removal methods

Figure 4.19(a) gives the additional chemical dose related to percentage of phosphorus removal. Figure 4.19(b) and 4.19(c) give the information of chemical dose related to amount of struvite and P precipitation. From Figure 4.19(a), the Pearl process could reach the optimal %P removal with a lower additional MgCl₂ than AirPrex. However, in Figure 4.19(b), the Pearl process produces less struvite than Airprex. It is because part of phosphorus removal from dewatering process with solid sludge. The amount of P in Airprex influent is much higher than the P in Pearl influence. For

the ferric precipitation, about 3500mg/L FeCl_3 is required to reach the optimal P removal. Figure 4.19(b) shows struvite precipitation decreasing with increasing FeCl_3 and there is no struvite for recovery at end. But from Figure 4.19(c), the amount of P recovery is close to 1000mg/L because most of phosphorus is precipitated as strengite.

CHAPTER 5. CONCLUSION

- At optimal conditions, the three P removal or recovery methods modeled, Airprex, Pearl® and ferric precipitation could all could achieve greater than 90% P removal.
- The Airprex technology treats the digested sludge from digester reactor. It effectively controls struvite precipitation because it is install just after digester reactor where nutrient is released. With the concentration of phosphorus in digested sludge reduced, the phosphorus in centrate and solid sludge which is produced in centrifuge after AirPrex process is reduced. So Airprex effectively reduces the P reload and improve sludge dewatering with low phosphorus level.
- The Pearl® technology treats centrate from a centrifuge dewatering process which contains 1% of the phosphorus in the digested sludge. This method focus on recovery struvite in highly pure crystalline pellets and reduce P reload from centrate. However, because Pearl® reactor installs after centrifuge, the problem of struvite accumulate between digester and dewatering process could not be control. In the centrifuge process, solid sludge is separated with centrate without P recovery, so the P in sludge does not reduce.
- Ferric chloride as a common chemical used to control struvite precipitation can reach 100% P precipitation. For control phosphorus and limit struvite precipitation, this method works well. But using ferric chloride, phosphorus that precipitates as ferric phosphate is not suitable for use as fertilizer. The ferric chloride is added in digested sludge after digester. The solid precipitate and separate in solid sludge through centrifuge process and the phosphorus in centrate is reduced. So this method also could reduce P reload, but increase sludge production as strengite solid.

- Airprex and method using ferric chloride treat digested sludge. The flow rate is much greater than centrate, so the amount of treatment aqueous and the additional chemical consumed are greater compared with the Pearl® process. In the other hand, for AirPrex, the available P for recovery is greater than Pearl®.
- Carbonate loss is high in the three methods modeled, because with aeration type conditions in an open reactor, the most carbon is lost as gas phase until it reach equilibrium saturation level. So when aqueous reach chemical equilibrium, rest of carbonate in sludge is similar.
- Visual MINTEQ is chemical equilibrium model. Even the solids which need long time period to precipitation are removed from solid list, the precipitation time for possible solid could not be control and model. So in real treatment plant, in certain treatment period, the amount of precipitated solid should be less than the results from model. But Virsual MINTEQ works on finding the optimal pH and additional chemicals dose.

REFERENCES

- Borgerding, Joseph. "Phosphate deposits in digestion systems." *Journal of the Water Pollution Control Federation* 44.5 (1972): 813-819.
- Buchanan, J. R., C. R. Mote, and R. B. Robinson. "Thermodynamics of struvite formation." *Transactions of the ASAE* 37.2 (1994): 617-621.
- Caravelli, Alejandro H., Edgardo M. Contreras, and Noemí E. Zaritzky. "Phosphorous removal in batch systems using ferric chloride in the presence of activated sludges." *Journal of hazardous materials* 177.1 (2010): 199-208.
- Çelen, Ipek, et al. "Using a chemical equilibrium model to predict amendments required to precipitate phosphorus as struvite in liquid swine manure." *Water Research* 41.8 (2007): 1689-1696.
- Correll, David L. "The role of phosphorus in the eutrophication of receiving waters: a review." *Journal of environmental quality* 27.2 (1998): 261-266.
- Doyle, James D., and Simon A. Parsons. "Struvite formation, control and recovery." *Water research* 36.16 (2002): 3925-3940.
- Forstner, Gerhard. "AirPrex: Biosolids Treatment Optimization Process with the option of Phosphate Recovery." March 2015. PowerPoint presentation.
- Hannes Herzal, Jan Stemann, Anders Nattorp, and Christian Adam "P-Recovery Technologies and Products." *FHNW Univerisity of Applied Sciences and Arts Northwestern Switzerland and BAM Federal Institute for Materials Research and Testing, Germany*. Nov 2015. PowerPoint presentation.
- Janssen, P. M. J., K. Meinema, and H. F. Van der Roest. *Biological phosphorus removal*. IWA publishing, 2002.

Kabbe, Christian. "Sustainable sewage sludge management fostering phosphorus recovery and energy efficiency." (2013).

Le Corre, Kristell S., et al. "Phosphorus recovery from wastewater by struvite crystallization: A review." *Critical Reviews in Environmental Science and Technology* 39.6 (2009): 433-477.

Mamais, Daniel, et al. "Determination of ferric chloride dose to control struvite precipitation in anaerobic sludge digesters." *Water Environment Research* 66.7 (1994): 912-918.

Marti, N., et al. "Phosphorus recovery by struvite crystallization in WWTPs: Influence of the sludge treatment line operation." *Water research* 44.7 (2010): 2371-2379.

Morse, G. K., et al. "Phosphorus removal and recovery technologies." *Science of the total environment* 212.1 (1998): 69-81.

Musvoto, E. V., M. C. Wentzel, and G. A. Ekama. "Integrated chemical–physical processes modelling—II. Simulating aeration treatment of anaerobic digester supernatants." *Water Research* 34.6 (2000): 1868-1880.

Rahaman, Md Saifur, et al. "Modeling phosphorus removal and recovery from anaerobic digester supernatant through struvite crystallization in a fluidized bed reactor." *Water research* 51 (2014): 1-10.

Seviour, Robert J., Takashi Mino, and Motoharu Onuki. "The microbiology of biological phosphorus removal in activated sludge systems." *FEMS Microbiology Reviews* 27.1 (2003): 99-127.

The Environmental Literacy Council. "Phosphorus Cycle." *The Environmental Literacy Council* (2015)

TÜRKER, MUSTAFA, and İPEK ÇELEN ERDEM. "Chemical equilibrium model of struvite precipitation from anaerobic digester effluents." *Turkish Journal of Engineering and Environmental Sciences* 35.1 (2011): 39-48.